

Structure of the nucleus of 1928+738

J. Roland¹, S. Britzen², E. Kun^{3,4}, G. Henri⁵, S. Lambert⁶ and A. Zensus²

¹ Institut d'Astrophysique, UPMC Univ Paris 06, CNRS, UMR 7095, 98 bis Bd Arago, 75014 Paris, France

² Max-Planck-Institut für Radioastronomie, Auf dem Hügel 69, Bonn 53121, Germany

³ Department of Experimental Physics, University of Szeged, Dóm tér 9, H-6720 Szeged, Hungary

⁴ Department of Theoretical Physics, University of Szeged, Tisza Lajos krt 84-86, H-6720 Szeged, Hungary

⁵ Laboratoire d'Astrophysique, Observatoire de Grenoble, 414, Rue de la Piscine, Domaine Universitaire, 38400 Saint-Martin d'Hères, France

⁶ Observatoire de Paris, SYRTE, CNRS, UPMC, CRGS, Paris, France

Received $j\ddot{c}$ / Accepted $j\ddot{c}$

ABSTRACT

Modeling of the trajectories of VLBI components ejected by the nucleus of 1928+738 shows the VLBI jet contains three families of trajectories, i.e. VLBI components are ejected from three different origins. The fit of components C1, C6 and C8 indicates that the nucleus of 1928+738 contains two binary black hole systems. The first binary black hole system is associated with the stationary components Cg and CS and is characterized by a radius $R_{bin,1} \approx 0.220$ mas; both black holes ejected VLBI components quasi regularly between 1990 and 2010. The second binary black hole system is not associated with stationary components and is characterized by a radius $R_{bin,2} \approx 0.140$ mas; it ejected only three VLBI components between 1994 and 1999. The two black hole systems are separated by ≈ 1.35 mas. We briefly discuss the consequences of the existence of binary black holes systems in radio quasars to make the link between radio quasars and GAIA.

Key words. Astrometry - individual: 1928+738 - Galaxies: jets

1. Introduction

VLBI observations of compact radio sources show that the ejection of VLBI components does not follow a straight line, but wiggles. These observations suggest a precession of the accretion disk. By studying the observed wiggles, several authors raised evidences that nuclei of extragalactic radio sources contain binary black hole (BBH) systems (see Britzen et al. (2001) for 0420-014, Lobanov & Roland (2005) for 3C 345, Roland et al. (2008) for 1803+784, Roland et al. (2013) for 1823+568 and 3C 279 and Roos et al. (1993), Kun et al. (2014), and this work for 1928+738). BBH systems can form when galaxies merge (Begelman et al. 1980) and the detection of BBH systems associated with nuclei of extragalactic radio sources can explain why extragalactic radio sources are associated with elliptical galaxies and why quasars (quasi stellar radio sources) represent about 5% of the quasi stellar objects (QSO) (Britzen et al. 2001). For a review concerning massive binary black holes systems, see Colpi & Dotti (2011).

A BBH system produces three perturbations of the VLBI ejection due to

1. the precession of the accretion disk,
2. the motion of the two black holes around the center of gravity of the BBH system, and
3. the possible motion of the BBH system around either a third black hole or another BBH system. This third perturbation produces a change of the VLBI jet direction. It is observed for 1928+738 (Fig 1), 3C 345 (Lister & Homan 2005) and 3C 454.3 (Lister et al. 2009a) for instance¹.

Send offprint requests to: J. Roland, e-mail: roland@iap.fr

¹ The BBH system can turn around the center of gravity of the galaxy, however the rotation period will be very large.

A BBH system induces several consequences, which are that

1. even if the angle between the accretion disk and the plane of rotation of the BBH system is zero, the ejection does not follow a straight line (due to the rotation of the black holes around the center of gravity of the BBH system),
2. the two black holes can have accretion disks with different angles with the plane of rotation of the BBH system and can eject VLBI components; in that case we observe two different families of trajectories, i.e. trajectories ejected from two different origins; a good example of a source showing two families of trajectories is 3C 279 (Roland et al. 2013), and
3. if the VLBI core is associated with one black hole, and if the VLBI component is ejected by the second black hole, there will be an offset between the VLBI core and the origin of the ejection of the VLBI component; this offset will correspond to the radius of the BBH system; a good example of a component ejected with a large offset from the VLBI core is component C5 of 3C 279 (Roland et al. 2013).

The existence of BBH systems impact several domains of astronomy and astrophysics. As indicated in Britzen et al. (2001) nuclei of extragalactic radio sources which contain BBH systems will be good candidates to be observed with low frequency gravitational wave detectors like eLISA. Britzen et al. (2001) showed that the typical life time of BBH systems associated with nuclei of extragalactic radio sources is between 5 to 10 billion years and during the final phase of the collapse there are observable during about 2.5 years. Britzen et al. (2001) also estimated that the frequency of the collapse of BBH systems associated with extragalactic radio sources will be about one collapse every 2.5 years.

The existence of BBH systems in nuclei of extragalactic radio sources has also consequences for the realization of celestial

frames. The absolute position of radio sources as measured by geodetic VLBI shows a standard deviation (rms) larger than 0.1 mas (see Sec. 8). This floor is partly due to the source structure, and constitutes a limit to the stability of a quasar-based celestial frame axes (e.g., Fey et al. (2009); Lambert (2013)).

In Sec. 2 we will recall the parameters of the model.

In Sec. 3 we will give the properties of the radio source 1928+738.

We found modeling and fitting the ejections of components C1, C5, C6, C7a, C8 and C9 that the nucleus of 1928+738 contains at least three black holes ejecting the VLBI components. We shown that the three black holes belong to two BBH systems, namely Cg-CS and BHC6-BH4. The black hole associated with the stationary component CS ejected components C1 and C9, the black hole associated with the stationary component Cg ejected components C8 and C7a, the third black hole BHC6 which ejected C6 and C5 is not detected in radio. In Sec. 4 we will explain to which family of trajectory belong the different components.

To find a precise determination of the two BBH systems:

1. we found the characteristics of the BBH system using the coordinates given by Kun et al. (2014),
2. we estimated the perturbation due to the slow rotation of the BBH system Cg-CS around the second BBH system BHC6-BH4 assuming $M_{BHC6} + M_{BH4} = (M_{CS} + M_{Cg})/10$ and corrected the coordinates given by (Kun et al. 2014) from this perturbation, finally
3. we used the corrected coordinates to find the final characteristics of the BBH system.

In Sec. 5 we give the solution of the fit of component C8 after correction of the slow rotation of the BBH system Cg-CS around the second BBH system BHC6-BH4.

In Sec. 6 we give the solution of the fit of component C1 after correction of the slow rotation of the BBH system Cg-CS around the second BBH system BHC6-BH4.

In Sec. 7 we give the solution of the fit of component C6 after correction of the slow rotation of the BBH system BHC6-BH4 around the second BBH system Cg-CS.

Finally, in Sec. 8 we study the consequences of BBH systems in nuclei of extragalactic radio sources to link radio positions obtained from VLBI observations and GAIA.

The fits of C1, C5, C6, C7a, C8 and C9 using the coordinates given by Kun et al. (2014) and the circular orbit corrections are given in the various appendices.

2. Parameters of the model

A VLBI component is a cloud of $e^- - e^+$ ejected relativistically. It corresponds to the relativistic beam in the two-fluid model. It follows the perturbed magnetic field lines, so its motion is not a ballistic motion. We will call x , y and z the coordinates of a point source component. For details concerning the geometry of the model, the two-fluid model, the perturbation of the VLBI ejection, the coordinates of the VLBI component see Roland et al. (2008) and Roland et al. (2013).

The possible free parameters of the model (for more details see Roland et al. (2013)). They are

- i_o the inclination angle,
- ϕ_o the phase of the precession at $t = 0$,
- ΔE the rotation angle in the plane perpendicular to the line of sight, also the asymptotic direction of the jet,

- Ω the opening angle of the precession cone,
- R_o the maximum amplitude of the perturbation,
- T_p the precession period of the accretion disk,
- T_d the characteristic time for the damping of the beam perturbation,
- M_1 the mass of the black hole ejecting the radio jet,
- M_2 the mass of the secondary black hole,
- γ_c the bulk Lorentz factor of the VLBI component,
- ψ_o the phase of the BBH system at $t = 0$,
- T_b the period of the BBH system,
- t_o the time of the origin of the ejection of the VLBI component,
- V_a the propagation speed of the perturbations,
- n_{rad} is the number of steps to describe the extension of the VLBI component along the beam,
- ΔW and ΔN the possible offsets of the origin of the VLBI component.

As M_1 and M_2 are free parameters, the ratio M_1/M_2 is also a free parameter.

The parameter V_a can be used to study the degeneracy of the solutions, so we can keep it constant to find the solution. The range of values that we study for parameter V_a is $0.001 \times c \leq V_a \leq 0.45 \times c^2$.

The parameter n_{rad} is known when the size of the VLBI component is known.

This means that, practically, the problem we have to solve is a 15 free parameter problem.

We have to investigate the different possible scenarios with regard to the sense of the rotation of the accretion disk and the sense of the orbital rotation of the BBH system. These possibilities correspond to $\pm \omega_p(t - z/V_a)$ and $\pm \omega_b(t - z/V_a)$. Because the sense of the precession is always opposite to the sense of the orbital motion (Katz 1997), we study the two cases denoted by $+-$ and $-+$, where we have $\omega_p(t - z/V_a)$, $-\omega_b(t - z/V_a)$ and $-\omega_p(t - z/V_a)$, $\omega_b(t - z/V_a)$, respectively (ω_p and ω_b are defined by $\omega_p = 2\pi/T_p$ and $\omega_b = 2\pi/T_b$).

3. Radio source 1928+738

The radio source S5 1928+738 is a core dominated quasar at a redshift of 0.302 (Lawrence et al. 1986). It is associated with a bright optical blazar which magnitude is $m_R \approx 15$ to 16 (Healey et al. 2008). The jet morphology is two-sided on kpc scales, the southern part being more pronounced (Murphy et al. 1993). On pc scales the source is one-sided. The map of 1928+738 (Fig. 1) shows that the VLBI jet turns after about 10 mas Lister & Homan (2005). Close to the nucleus the ejection direction is characterized by $\Delta E \approx 163^\circ$ and after about 10 mas, the VLBI jet turns and has an asymptotic direction characterized by $\Delta E \approx 182^\circ$ which corresponds to the large scale jet direction observed with the VLA (Murphy et al. 1993). As mentioned in Sec. 1, the VLBI jet turn could be an indication that the nucleus of 1928+738 contains either three black holes or two BBH systems. We will see that components C5 and C6 are ejected by either a third black hole or a second BBH system, so we will have to estimate the influence of the slow rotation of the BBH system Cg-CS around the mass ejecting C5 and C6 and we will have to correct the coordinates given by Kun et al. (2014) from this perturbation to obtain the precise characteristics of the BBH system Cg-CS.

VLBI observations of S5 1928+738 used in the present work were taken between 1994.67 and 2013.06 at 15 GHz in the

² We limit ourselves to non relativistic hydrodynamics in this model.

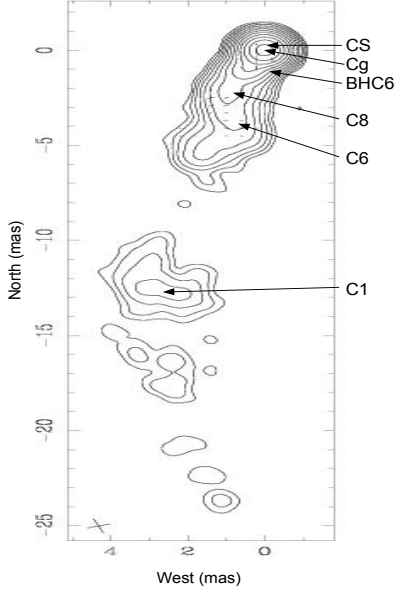


Fig. 1. VLBI image of S5 1928+738 observed 28 Aug 2003 and obtained by Lister & Homan (2005). The VLBI jet turns after about 10 mas and the asymptotic direction is characterized by $\Delta E \approx 182^\circ$ corresponds to the direction of the large scale jet observed with the VLA (Murphy et al. 1993). This long term turn is characteristic of the slow rotation of the BBH system around a third black hole or a second BBH system. We indicated the positions of the two stationary components Cg and CS which are associated with the two black holes of the BBH system Cg-CS, the position of the black hole BHC6 which ejected components C5, C6 and C7b and finally the positions of components C1, C6 and C8 which ejections have been fitted.

framework of the MOJAVE Survey Lister et al. (2009a) and Lister et al. (2009b). Kun et al. (2014) decomposed the brightness distribution of the jet for its components by using the Caltech DIFMAP software package (Shepherd 1997). The core and the jet components were fitted by circular Gaussian. For details about the error calculation and component identification see Kun et al. (2014). We will consider the VLBI core is associated with component Cg; Kun et al. (2014) consider that the VLBI core is associated with component CS. So the original coordinates of Kun et al. (2014) have been corrected to take into account this new origin. In this article when we refer to the coordinates of Kun et al. (2014), they correspond to the coordinates corrected to take into account the origin Cg.

The kinematics of the jet reveals superluminal motion of its components. The jet components show outward motion, except the northernmost component, component CS, which is observed at a quasi-stationary position compared to the core. 16 components appear at 15 GHz, averagely 10-14 in one epoch. The separation from the core of the different components is shown in Fig 2. The radio map of 1928+738, observed 28 Aug 2003, is showed in Fig. 1.

The redshift of the source is $z_s \approx 0.302$, and using for the Hubble constant $H_o \approx 71$ km/s/Mpc, the luminosity distance of the source is $D_l \approx 1552$ Mpc and the angular distance is $D_a = D_l / (1 + z)^2$. Thus $1 \text{ mas} \approx 4.44 \text{ pc}$.

Observations were performed at 15 GHz and the beam size is mostly circular and equal to $Beam \approx 0.5 \text{ mas}$. We adopted as minimum values of the error bars the values $(\Delta W)_{min} \approx Beam/15 \approx 34 \mu\text{as}$ and $(\Delta N)_{min} \approx Beam/15 \approx 34 \mu\text{as}$ for the

west and north coordinates, i.e., when the error bars obtained from the VLBI data reduction were smaller than $(\Delta W)_{min}$ or $(\Delta N)_{min}$, they were enlarged to the minimum values (see Roland et al. (2013) for details concerning this choice).

It has been suggested by Lister & Homan (2005) that the minimum values for the error bars should be $\approx Beam/5$, however Roland et al. (2013) shown that the correct minimum values for the error bars adopted at 15 GHz, are given by

$$Beam/15 \leq \Delta_{min} \leq Beam/12. \quad (1)$$

The fit of VLBI coordinates of components of 3C 345 (work in progress) indicates that the adopted values for the minimum values of the error bars, using equation (1), are correct for frequencies between 8 GHz and 22 GHz. At lower frequencies, the minimum values may be higher than $Beam/12$ due to strong opacity effects and at 43 GHz, the minimum values are also probably higher ($\approx 20 \mu\text{as}$).

There are two important points concerning the minimum values used for the error bars:

1. The minimum values are chosen empirically, but the adopted values are justified a posteriori by comparing of the value of χ^2 of the final solution and the number of constraints used to make the fit. Indeed, the reduced χ^2 has to be close to 1.
2. The adopted minimum value of the error bars also includes typical errors due to opacity effects, which shift the measured position at different frequencies (Lobanov 1998).

We will model and fit the coordinates $W(t)$ and $N(t)$ of components C8, C1 and C6 which, as our modeling shows, have been ejected respectively by the three different black holes Cg, CS and BHC6 (Fig. 2, Sec. 5, Sec. 6, and Sec. 7) and to check the consistency of the model found, we fit the coordinates of components C7a, C9 and C5 which have been ejected respectively by Cg, CS and BHC6 (see Sec. C, Sec. F and Sec. I).

The model and the fit of components C8, C1, C6, C7a, C9 and C5 have been obtained with the sense of the rotation of the accretion disks $-\omega_p(t-z/V_a)$ and the sense of the orbital rotation of the BBH systems $+\omega_b(t-z/V_a)$.

4. Families of trajectories in the VLBI jet

Modeling the ejections of components C8, C1, C6, C7a, C9 and C5, we found that the VLBI jet is a blend of three families of trajectories, i.e. the nucleus of 1928+738 contains at least three black holes ejecting VLBI components. The first one corresponds to the VLBI components ejected by CS, the second one corresponds to the VLBI components ejected by Cg and the third one corresponds to the VLBI components ejected by the third black hole, we will call BHC6.

In this section we will indicate to which family of trajectory belong the components. When the fit of the component has not been done we indicate the possible membership of the component using the trajectories, the distance from the core variations and the flux densities variations, and we give the time origin of the ejection. We use the data and component identifications from Kun et al. (2014).

Component C1: Modeling the ejection of C1, we found after the circular orbit correction that the mass ratio M_{CS}/M_{Cg} is $M_{CS}/M_{Cg} \approx 1/3$ indicating that component C1 cannot be ejected by the same black hole responsible for the ejection of component C8, i.e. C1 is not ejected by Cg but by CS (see Sec. 6, Fig D.2, Fig D.3 and Fig. 3). So, C1 define the first family of trajectories and has been ejected by the black hole associated with CS

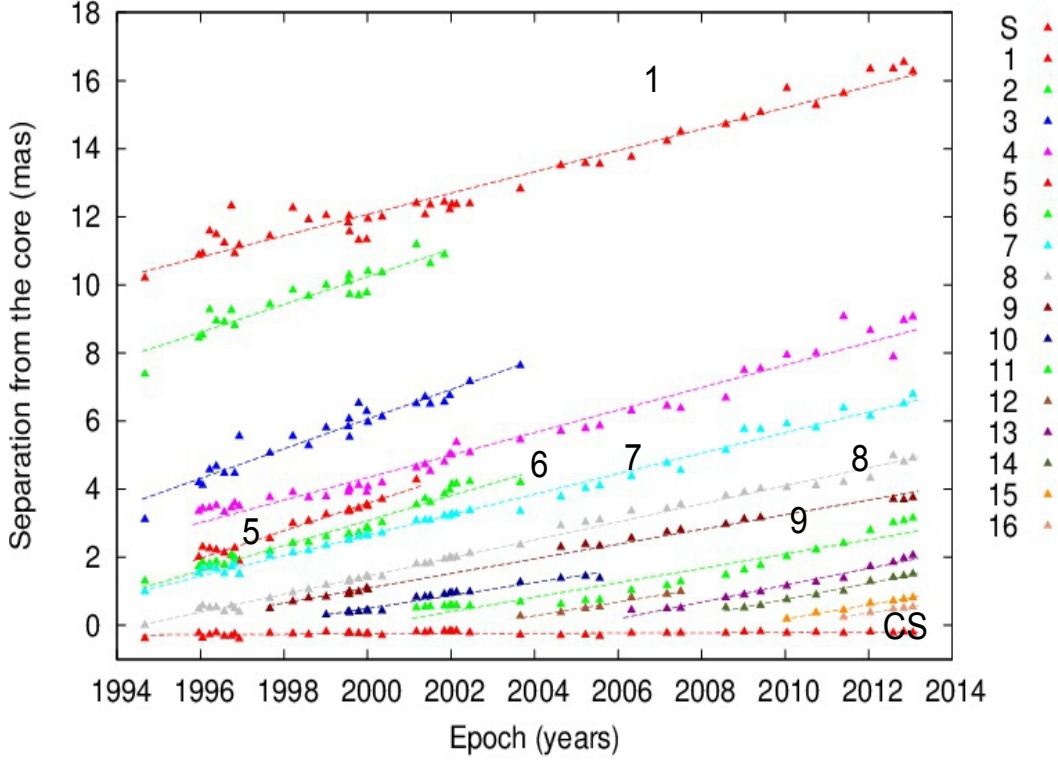


Fig. 2. Separation from the core for the different VLBI components obtained by Kun et al. (2014) for the source 1928+738 using from MOJAVE data (Lister et al. 2009b). We fitted components C1, C6 and C8 which have been ejected respectively by black holes Cg, CS and BHC6 and to check the consistency of the model found we fitted components C7a, C9 and C5 which have been ejected respectively by black holes Cg, CS and BHC6.

which coordinates are $X_{CS} \approx -0.07$ mas and $Y_{CS} \approx +0.21$ mas and $t_o \approx 1967$.

Component C2: follows the same trajectory than C1, so has probably been ejected by CS, and $t_o \approx 1975$ (Fig. 3).

Component C3: follows the same trajectory than C8, so has probably been ejected by the black hole associated with Cg which coordinates are $X_{CS} = 0.0$ mas and $Y_{CS} + 0.0$ mas and $t_o \approx 1986$ (Fig. 3).

Component C4: is possibly a blend of two components C4a and C4b. The beginning of the trajectory, C4a i.e. from 1996 to 2008.6, is the same than C8, so it has probably been ejected by Cg and $t_o \approx 1987$. The end of the trajectory, C4b i.e. the last eight points from 2008.9 to 2013.1, is the same than C1, and $t_o \approx 1990$ (Fig. 3).

Component C5: follows the same trajectory than C6 which is different from C1 and C8. To check that component C5 belongs to the family of components ejected by the black hole BHC6 and the consistency of the model found, we used the characteristics of the BBH system BHC6-BH4 and the characteristics of the geometrical parameters of the trajectory of C6, to fit the coordinates of components C5 (see Sec. I, Fig. I.1 and Fig. 4). So, C5 is ejected by the black hole BHC6, so it belongs to the third family of trajectory, and $t_o \approx 1991$.

Component C6 : define the third family of trajectories, i.e. is ejected by the third black hole, BHC6, which coordinates

are $X_{BHC6} \approx -0.10$ mas and $Y_{BHC6} \approx -1.30$ mas (see Sec. 7, Fig. G.3, Fig. G.4 Fig. 4 and Fig. 6), and $t_o \approx 1994.5$.

Component C7 : is a blend of two components C7a and C7b. The beginning of the trajectory (from 1994.5 to 2002.5), C7a, is the same than C8. To check that component C7a belongs to the family of components ejected by the black hole Cg and the consistency of the model found, we used the characteristics of the BBH system Cg-CS and the characteristics of the geometrical parameters of the trajectory of C8, to fit the coordinates of components C7a (see Sec. C, Fig. C.1 and Fig. 3). So, C7a belongs to the second family of trajectories, i.e. has been ejected by Cg and $t_o \approx 1992$. The end of the trajectory, C7b, is the same that C5 and C6, so C7b has been probably ejected by BHC6, and $t_o \approx 1998.5$ (Fig. 4).

Component C8: Modeling the ejection of C8, we found after the circular orbit correction that the mass ratio M_{Cg}/M_{CS} is $M_{Cg}/M_{CS} \approx 3$ and there no offset of the origin of the ejection, indicating that component C8 cannot be ejected by the same black hole responsible for the ejection of component C1, i.e. C8 is not ejected by CS but by Cg (see Sec. 5, Fig. A.2, Fig. A.3 and Fig. 3). So, C8 define the second family of trajectories and has been ejected by Cg and $t_o \approx 1993.8$.

Component C9: follows the same trajectory than C1. To check that component C9 belongs to the family of components ejected by the black hole CS and the consistency of the model found, we used the characteristics of the BBH system Cg-CS and

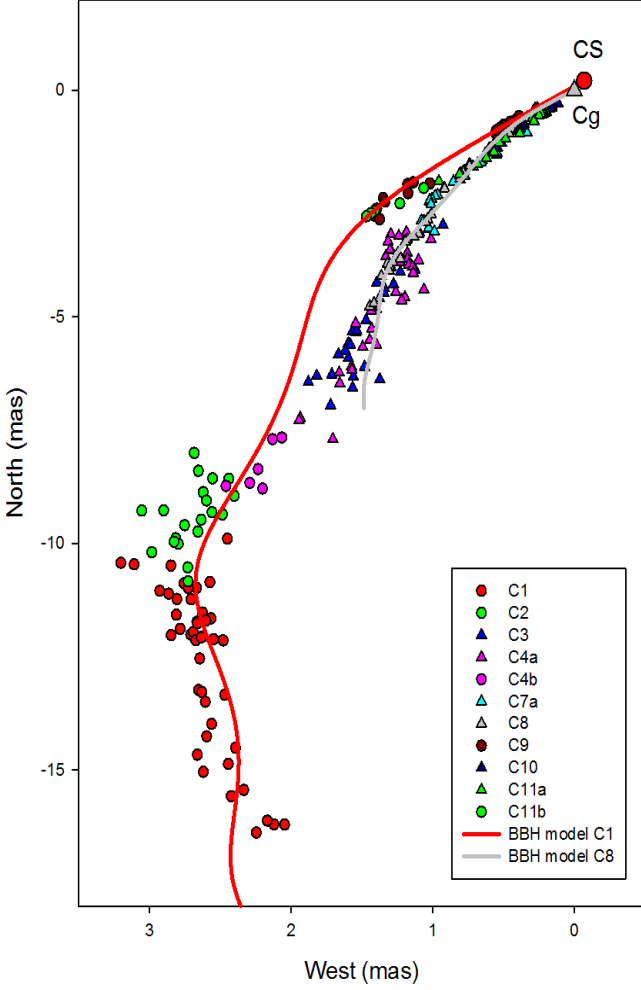


Fig. 3. The two families of trajectories, associated with the VLBI components ejected by CS and the VLBI components ejected by Cg. The two families separate clearly after 1 mas. Components C1 and C9 have been ejected by CS and components C2, C4b and C11b have been probably ejected by CS. They form the first family of VLBI trajectories. Components C8 and C7a have been ejected by Cg and components C3, C4a, C10 and C11a have been probably ejected by Cg. They form the second family of VLBI trajectories. The VLBI coordinates are taken from Kun et al. (2014).

the characteristics of the geometrical parameters of the trajectory of C1, to fit the coordinates of components C9 (see Sec. F, Fig. F.1 and Fig. 3). So, C9 belongs to the first family of trajectories, i.e. has been ejected by CS, and $t_o \approx 1995$.

Component C10: follows the same trajectory than C8, has been probably ejected by Cg, and $t_o \approx 1997.8$ (Fig. 3).

Component C11: is a blend of two components, C11a and C11b. The beginning of the trajectory, C11a, follows the same trajectory than C8, has been probably ejected by Cg, and $t_o \approx 1998$ (Fig. 3). The end of the trajectory, C11b, follows the same trajectory than C9, has been probably ejected by CS, and $t_o \approx 2003$ (Fig. 3).

For the next components, their trajectories are not long enough to determine if their trajectories are similar to C1 or C8. However, none of them are ejected by BHC6.

Component C12: has been ejected by Cg or CS, and $t_o \approx 2002.5$.

Component C13: may be a blend of two components that have been ejected by Cg or CS, and $2005 \leq t_o \leq 2007$.

Component C14: has been ejected by Cg or CS, and $t_o \approx 2006.5$.

Component C15: has been ejected by Cg or CS, and $t_o \approx 2009$.

Component C16: has been ejected by Cg or CS, and $t_o \approx 2010$.

We found that the VLBI components follow three different families of trajectories, i.e. the nucleus of 1928+738 contains at least three black holes. However, as we will see, the fit of the ejection of C6 cannot be explained simply a third black hole but indicates that C6 is ejected by a second BBH system. So the nucleus of 1928+738 contains 2 BBH systems. Let us call

1. Cg and CS the two black holes of the first BBH system and
2. BHC6 and BH4 the two black holes of the second BBH system.

As indicated in Sec. 1 the BBH system Cg-CS turns around the second BBH system BHC6-BH4, so we will have to correct this slow rotation to make a precise determination of the two BBH systems parameters.

We will model and fit the coordinates of components C8, C1 and C6 and we will be able to deduce the characteristics of the two BBH systems (see Sec. 5, Sec. 6, Sec. 7 and Sec. 8). To check the consistency of the model found, we will use the characteristics of the two BBH systems and the geometrical parameters of the trajectories of C8, C1 and C6 to fit the coordinates of components C7a, C9 and C5 which have been ejected respectively by Cg, CS and BHC6 (see Sec. C, Sec. F and Sec I).

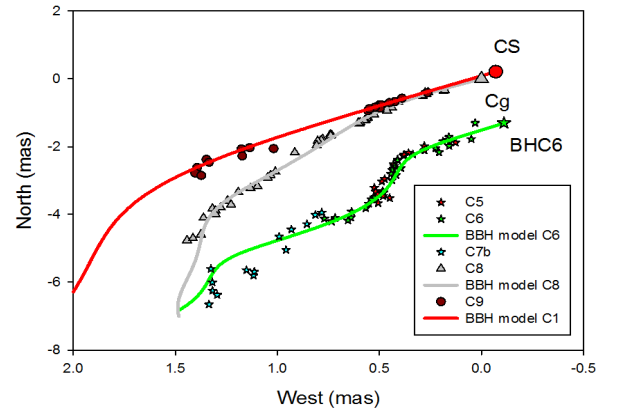


Fig. 4. The family of trajectories, associated with the VLBI components ejected by the third black hole BHC6. Components C5 and C6, have been ejected by BHC6 and C7b has been probably ejected by BHC6. They form the third family of VLBI trajectories. The VLBI coordinates are taken from Kun et al. (2014).

We plotted in Fig. 5 the time origin of the component ejected by three black holes of the nucleus of 1928+738 during the period from 1985 to 2015. We find that

- there is no obvious periodicity in the ejection time of the VLBI components,
- black hole BHC6, ejected components only during the period from 1991 to 1999,
- black hole Cg ejects about two time more components than black hole CS.

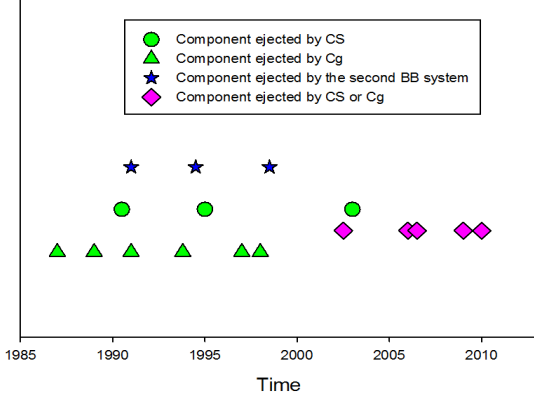


Fig. 5. Time origin of the component ejected by the three black holes of the nucleus of 1928+738 during the period from 1985 to 2015.

5. Fit of component C8

To obtain a precise determination of the characteristics of the BBH system ejecting component C8,

1. we found the characteristics of the BBH system Cg-CS using the coordinates of C8 given by Kun et al. (2014), see Sec. A,
2. we estimated the perturbation due to the slow rotation of the BBH system Cg-CS around the second BBH system BHC6-BH4 assuming $M_{BHC6} + M_{BH4} = (M_{CS} + M_{Cg})/10$ and corrected the coordinates given by (Kun et al. 2014) from this perturbation, see details in Sec. B, finally
3. we used the corrected coordinates to find the final characteristics of the BBH system Cg-CS.

Here we present the solution to the fit of the coordinates of C8 which have been corrected from the slow motion of the BBH system Cg-CS around the BBH system BHC6-BH4.

The main characteristics of the BBH system ejecting C8 are that

- the VLBI component C8 is ejected by the VLBI core, i.e. component Cg (there is no indication of an offset of the origin of the ejection),
- the two black holes are associated with the components CS and Cg,
- the radius of the BBH system is $R_{bin} \approx 220 \mu as \approx 0.98 pc$,
- the ratio M_{Cg}/M_{CS} is ≈ 3 , which is the inverse of the mass ratio found fitting the coordinates of C1 (Sec. 6) and
- the ratio T_p/T_b is ≈ 107 .

The ratio M_{Cg}/M_{CS} is a free parameter of the model and is determined by the fit of the coordinates of C8.

We find also that

- the inclination angle is $i_o \approx 18.5^\circ$,
- the asymptotic ejection direction is $\Xi \approx 165^\circ$,
- the angle between the accretion disk and the rotation plane of the BBH system is $\Omega \approx 2.7^\circ$,
- the bulk Lorentz factor of the VLBI component is $\gamma_c \approx 5.9$, and
- the origin of the ejection of the VLBI component is $t_o \approx 1993.8$.

Compared to the first solution found in Sec. A, this new solution is characterized by a smaller inclination angle, a smaller mass ratio M_{Cg}/M_{CS} , a smaller angle between the accretion disk and the rotation plane of the BBH system and an asymptotic direction of the VLBI jet, $\Delta\Xi \approx 165^\circ$ indicating that the long term turn of the VLBI jet observed at about 10 mas is due to the rotation of the BBH system Cg-CS around the BBH system BHC6-BH4.

5.1. Determining the family of solutions

For the inclination angle previously found, i.e., $i_o \approx 18.5^\circ$, $T_p/T_b \approx 107$, $M_{Cg}/M_{CS} \approx 3$, and $R_{bin} \approx 220 \mu as$, we gradually varied V_a between 0.001 c and 0.45 c. The function $\chi^2(V_a)$ remained constant, indicating a degeneracy of the solution. We deduced the range of variation of the BBH system parameters. They are given in Table 1.

Table 1 : Ranges for the BBH system parameters ejecting C8

V_a	0.001 c	0.45 c
$T_p(V_a)$	≈ 17800000 yr	≈ 21400 yr
$T_b(V_a)$	≈ 166000 yr	≈ 199 yr
$(M_{Cg} + M_{CS})(V_a)$	$\approx 3 \cdot 10^5 M_\odot$	$\approx 2.0 \cdot 10^{11} M_\odot$

Table 1 provides the range of the BBH system parameters ejecting C8. To obtain the final range of the two BBH systems Cg-CS and BHC6-BH4 one has to make the intersection of the ranges of BBH systems parameters found after the fits of C8, C1 and C6 (this is done in Sec. 8).

5.2. Determining the size of the accretion disk

From the knowledge of the mass ratio $M_{Cg}/M_{CS} \approx 3$ and the ratio $T_p/T_b \approx 107$, we calculated in the previous section the mass of the ejecting black hole M_{Cg} , the orbital period T_b , and the precession period T_p for each value of V_a .

The rotation period of the accretion disk, T_{disk} , is given by (Britzen et al. 2001)

$$T_{disk} \approx \frac{4}{3} \frac{M_{Cg} + M_{CS}}{M_{CS}} T_b \frac{T_b}{T_p}. \quad (2)$$

Thus we calculated the rotation period of the accretion disk, and assuming that the mass of the accretion disk is $M_{disk} \ll M_{Cg}$, the size of the accretion disk R_{disk} is

$$R_{disk} \approx \left(\frac{T_{disk}^2}{4\pi^2} GM_{Cg} \right)^{1/3}. \quad (3)$$

We found that the size of the accretion disk does not depend on V_a and is $R_{disk} \approx 0.027 mas \approx 0.120 pc$.

6. Fit of component C1

To obtain a precise determination of the characteristics of the BBH system ejecting component C1,

1. we found the characteristics of the BBH system Cg-CS using the coordinates of C1 given by Kun et al. (2014), see Sec. D,
2. we estimated the perturbation due to the slow rotation of the BBH system Cg-CS around the second BBH system BHC6-BH4 assuming $M_{BHC6} + M_{BH4} = (M_{CS} + M_{Cg})/10$ and corrected the coordinates given by (Kun et al. 2014) from this perturbation, see details in Sec. E, finally
3. we used the corrected coordinates to find the final characteristics of the BBH system Cg-CS.

Here we present the solution to the fit of the coordinates of C1 which have been corrected from the slow motion of the BBH system Cg-CS around the BBH system BHC6-BH4.

The main characteristics of the BBH system ejecting C1 are that

- the VLBI component C1 is not ejected by the VLBI core Cg, but by component CS (there is a weak indication of an offset of the origin of the VLBI ejection in the direction of CS, this weak indication is due to the lack of observations of C1 for the beginning of the trajectory),
- the coordinates of CS are $X_{CS} \approx -0.07$ mas and $Y_{CS} \approx +0.21$ mas,
- the radius of the BBH system is $R_{bin} \approx 220 \mu\text{as} \approx 0.98 pc$,
- the ratio M_{CS}/M_{Cg} is $\approx 1/3$, which is the inverse of the mass ratio found fitting the coordinates of C8 (Sec. 5) and
- the ratio T_p/T_b is ≈ 31 .

The ratio M_{CS}/M_{Cg} is a free parameter of the model and the value $M_{CS}/M_{Cg} \approx 1/3$ comes from the fit of the coordinates of C1. The fact that the fit of C1 provides a mass ratio $M_{CS}/M_{Cg} \approx 1/3$ which is the inverse of the mass ratio $M_{Cg}/M_{CS} \approx 3$ obtained from the fit of component C8 shows that components C1 and C8 are not ejected by the same black hole. This result shows the consistency of the method and it is remarkable to find this result with only parts of the complete trajectories of C1 and C8.

We find that

- the inclination angle is $i_o \approx 19^\circ$,
- the asymptotic ejection direction is $\Xi \approx 162^\circ$,
- the angle between the accretion disk and the rotation plane of the BBH system is $\Omega \approx 2.4^\circ$,
- the bulk Lorentz factor of the VLBI component is $\gamma_c \approx 10.2$, and
- the origin of the ejection of the VLBI component is $t_o \approx 1966.2$.

Compared to the first solution found in Sec. D, this new solution is characterized by a smaller inclination angle, a smaller angle between the accretion disk and the rotation plane of the BBH system, and an asymptotic direction of the VLBI jet, $\Delta\Xi \approx 162^\circ$ indicating that the long term turn of the VLBI jet observed at about 10 mas is due to the rotation of the BBH system Cg-CS around the BBH system BHC6-BH4.

6.1. Determining the family of solutions

For the inclination angle previously found, i.e., $i_o \approx 19^\circ$, $T_p/T_b \approx 31$, $M_{CS}/M_{Cg} \approx 1/3$, and $R_{bin} \approx 220 \mu\text{as}$, we gradually varied V_a between 0.001 c and 0.45 c. The function $\chi^2(V_a)$

remained constant, indicating a degeneracy of the solution. We deduced the range of variation of the BBH system parameters. They are given in Table 2.

Table 2 : Ranges for the BBH system parameters ejecting C1

V_a	0.001 c	0.45 c
$T_p(V_a)$	≈ 6700000 yr	≈ 8100 yr
$T_b(V_a)$	≈ 220000 yr	≈ 265 yr
$(M_{Cg} + M_{CS})(V_a)$	$\approx 1.7 \cdot 10^5 M_\odot$	$\approx 1.2 \cdot 10^{11} M_\odot$

Table 2 provides the range of the BBH system parameters ejecting C1. To obtain the final range of the two BBH systems Cg-CS and BHC6-BH4 one has to make the intersection of the ranges of BBH systems parameters found after the fits of C8, C1 and C6 (this is done in Sec. 8).

6.2. Determining the size of the accretion disk

From the knowledge of the mass ratio $M_{CS}/M_{Cg} \approx 1/3$ and the ratio $T_p/T_b \approx 31$, we calculated in the previous section the mass of the ejecting black hole M_{CS} , the orbital period T_b , and the precession period T_p for each value of V_a .

The rotation period of the accretion disk, T_{disk} , is given by (2). Thus we calculated the rotation period of the accretion disk, and assuming that the mass of the accretion disk is $M_{disk} \ll M_{CS}$, the size of the accretion disk is given by (3). We found that the size of the accretion disk, does not depend on V_a and is $R_{disk} \approx 0.021 \text{ mas} \approx 0.093 pc$.

7. Fit of component C6

The component C6 is not ejected by CS or Cg but is ejected by a third black hole which belongs to a second BBH system. Let us call BHC6 the black hole ejecting component C6 and BH4 the fourth black hole. If we assume that C6 is ejected by a single black hole, we applied the precession model and we studied the solution $\chi^2(i_o)$ in the interval $2^\circ \leq i_o \leq 50^\circ$, we found that

1. there exist solutions with $\gamma < 30$ only in the interval $2^\circ \leq i_o \leq 17^\circ$ (see Fig. G.1) and
2. the solution with $\gamma < 30$ is a mirage solution, i.e. the curve $\chi^2(i_o)$ is convex and it does not show a minimum; moreover the bulk Lorentz factor γ diverges when $i_o \rightarrow 17^\circ$ (see Fig. G.2).

see more details in Sec. G.

To obtain a precise determination of the characteristics of the BBH system ejecting component C6,

1. we found the characteristics of the BBH system BHC6-BH4 using the coordinates of C6 given by (Kun et al. 2014), see Sec. G,
2. we estimated the perturbation due to the slow rotation of the BBH system BHC6-BH4 around the second BBH system Cg-CS assuming $M_{BHC6} + M_{BH4} = (M_{CS} + M_{Cg})/10$ and corrected the coordinates given by (Kun et al. 2014) from this perturbation, see details in Sec. H, finally
3. we used the corrected coordinates to find the final characteristics of the BBH system BHC6-BH4.

The main characteristics of the solution of the BBH system ejecting C6 are that

- the coordinates of BHC6 are $X_{BHC6} \approx -0.11$ mas and $Y_{BHC6} \approx -1.30$ mas (assuming that the origin is associated with Cg),

- none of the two black holes are associated with a stationary VLBI component, i.e. they are not strong sources,
- the radius of the BBH system is $R_{bin} \approx 140 \mu\text{as} \approx 0.62 \text{ pc}$,
- calling M_{BHC6} the mass of the black hole ejecting C6 and M_{BH4} the mass of the other black hole, the ratio M_{BHC6}/M_{BH4} is ≈ 0.12 , and
- the ratio T_p/T_b is ≈ 50 .

We find that

- the inclination angle is $i_o \approx 23^\circ$,
- the asymptotic ejection direction is $\Xi \approx 165^\circ$,
- the angle between the accretion disk and the rotation plane of the BBH system is $\Omega \approx 1.9^\circ$,
- the bulk Lorentz factor of the VLBI component is $\gamma_c \approx 5.7$, and
- the origin of the ejection of the VLBI component is $t_o \approx 1994.5$.

Compared to the first solution found in Sec. G, this new solution is characterized by a similar inclination angle, a smaller angle between the accretion disk and the rotation plane of the BBH system, and a smaller mass ratio M_{BHC6}/M_{BH4} .

7.1. Determining the family of solutions

For the inclination angle previously found, i.e., $i_o \approx 23^\circ$, $T_p/T_b \approx 50$, $M_{BHC6}/M_{BH4} \approx 0.12$, and $R_{bin} \approx 140 \mu\text{as}$, we gradually varied V_a between 0.001 c and 0.45 c. The function $\chi^2(V_a)$ remained constant, indicating a degeneracy of the solution. We deduced the range of variation of the BBH system parameters. They are given in Table 3.

Table 3 : Ranges for the BBH system parameters ejecting C6

V_a	0.001 c	0.45 c
$T_p(V_a)$	$\approx 4300000 \text{ yr}$	$\approx 5200 \text{ yr}$
$T_b(V_a)$	$\approx 84600 \text{ yr}$	$\approx 103 \text{ yr}$
$(M_{BHC6} + M_{BH4})(V_a)$	$\approx 2.9 \cdot 10^5 M_\odot$	$\approx 2.0 \cdot 10^{11} M_\odot$

Table 3 provides the range of the BBH system parameters ejecting C6. To obtain the final range of the two BBH systems Cg-CS and BHC6-BH4 one has to make the intersection of the ranges of BBH systems parameters found after the fits of C8, C1 and C6 (this is done in Sec. 8).

7.2. Determining the size of the accretion disk

From the knowledge of the mass ratio $M_{BHC6}/M_{BH4} \approx 0.12$ and the ratio $T_p/T_b \approx 50$, we calculated in the previous section the mass of the ejecting black hole M_{BHC6} , the orbital period T_b , and the precession period T_p for each value of V_a .

The rotation period of the accretion disk, T_{disk} , is given by (2). Thus we calculated the rotation period of the accretion disk, and assuming that the mass of the accretion disk is $M_{disk} \ll M_{BHC6}$, the size of the accretion disk is given by (3). We found that the size of the accretion disk, does not depend on V_a and is $R_{disk} \approx 0.006 \text{ mas} \approx 0.027 \text{ pc}$.

8. Discussion and conclusion

Modeling the ejections of components C8, C1, C6, C7a, C9 and C5, we found that the VLBI components follow three different families of trajectories, i.e. the nucleus of 1928+738 contains at least three black holes. The fit of the ejection of C6 cannot be

explained simply by a third black hole but indicates that C6 is ejected by a second BBH system, so the nucleus of 1928+738 contains 2 BBH systems.

To determine precisely the characteristics of the BBH systems

1. we found the characteristics of the BBH system ejecting a component using the coordinates of the component given by (Kun et al. 2014),
2. we estimated the perturbation due to the slow rotation of the BBH system ejecting the component around the second BBH system assuming $M_{BHC6} + M_{BH4} = (M_{CS} + M_{Cg})/10$ and corrected the coordinates given by (Kun et al. 2014) from this perturbation, finally
3. we used the corrected coordinates to find the final characteristics of the BBH system.

The characteristics of the two BBH systems are

- the distance between the two BBH systems is $\approx 1.35 \text{ mas} \approx 6.0 \text{ pc}$,
- the first BBH system is constituted by the components Cg and CS,
- the radius of the BBH system is $R_{bin,1} \approx 220 \mu\text{as} \approx 0.98 \text{ pc}$,
- the mass ratio of the two black holes is $M_{Cg} = 3 \times M_{CS}$,
- the coordinates of the two black holes are $X_{Cg} = 0$, $Y_{Cg} = 0$ (by definition) and $X_{CS} \approx -70 \mu\text{as}$, $Y_{CS} \approx +210 \mu\text{as}$,
- the two black holes of the second BBH system, namely BHC6 and BH4 are not associated with stationary VLBI components, i.e. they are not strong radio sources,
- the radius of the BBH system is $R_{bin,2} \approx 140 \mu\text{as} \approx 0.62 \text{ pc}$,
- the mass ratio of the two black holes is $M_{BHC6} = 0.12 \times M_{BH4}$ and
- the coordinates of the black hole BHC6 is $X_{BHC6} \approx -100 \mu\text{as}$, $Y_{CS} \approx -1300 \mu\text{as}$ and the coordinates of BH4 are unknown.

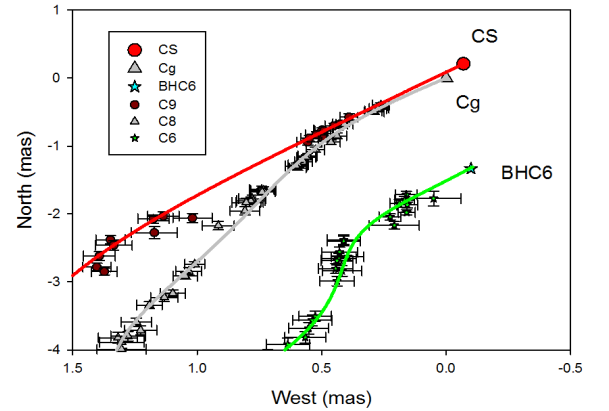


Fig. 6. Structure of the nucleus of 1928+738. The nucleus of 1928+738 contains two BBH systems separated by $\approx 1.35 \text{ mas} \approx 6 \text{ pc}$. The first BBH system is constituted by components Cg and CS and has a size $R_{bin,1} \approx 220 \mu\text{as} \approx 0.98 \text{ pc}$. The second BBH system is constituted by BHC6 and BH4 which are not detected in radio and has a size $R_{bin,2} \approx 140 \mu\text{as} \approx 0.62 \text{ pc}$. The position of BH4 is unknown.

We found that the inclination angle is between $i_o \approx 18.5^\circ$ and $i_o \approx 23.5^\circ$.

Combining the constraints obtained using the fits of components C1, C6 and C8, i.e. making the intersection of the ranges of the BBH systems parameters given in Tables 1, 2 and 3, we can deduce the characteristics of the BBH systems associated with the nucleus of 1928+738. They are

- the total mass of the BBH system Cg-CS is $3 \cdot 10^6 M_{\odot} \leq M_{Cg} + M_{CS} \leq 1.2 \cdot 10^{11} M_{\odot}$,
- the period of the BBH system Cg-CS is $265 \text{ yr} \leq T_{bin} \leq 52200 \text{ yr}$,
- the size of the accretion disk around Cg is $R_{disk,Cg} \approx 0.027 \text{ mas} \approx 0.12 \text{ pc}$ and the rotation period of the disk is $13.2 \text{ yr} \leq T_{disk,Cg} \leq 2590 \text{ yr}$,
- the size of the accretion disk around CS is $R_{disk,CS} \approx 0.021 \text{ mas} \approx 0.093 \text{ pc}$ and the rotation period of the disk is $15.5 \text{ yr} \leq T_{disk,CS} \leq 3040 \text{ yr}$,
- the total mass of the BBH system BHC6-BH4 is $3 \cdot 10^5 M_{\odot} \leq M_{BHC6} + M_{BH4} \leq 1.2 \cdot 10^{10} M_{\odot}$,
- the period of the BBH system BHC6-BH4 is $420 \text{ yr} \leq T_{bin} \leq 84600 \text{ yr}$,
- the size of the accretion disk around BHC6 is $R_{disk,Cg} \approx 0.006 \text{ mas} \approx 0.027 \text{ pc}$ and the rotation period of the disk is $12.4 \text{ yr} \leq T_{disk,Cg} \leq 2500 \text{ yr}$,

Combining the constraints obtained using the fits of components C1, C6 and C8 reduce the range of the parameters obtained for each fit done separately.

Roos et al. (1993) assumed that the mass of the nucleus was $\approx 10^8 M_{\odot}$ and Kelly & Bechtold (2007) estimated the mass of the nucleus to be $\approx 8 \cdot 10^8 M_{\odot}$. So, if we assume $M_{Cg} + M_{CS} \approx 8 \cdot 10^8 M_{\odot}$, we have $M_{Cg} \approx 6 \cdot 10^8 M_{\odot}$ and $M_{CS} \approx 2 \cdot 10^8 M_{\odot}$. We find that the orbital period of the BBH system (Cg-CS) is $T_{bin} \approx 3195 \text{ yr}$, and the rotation periods of the accretion disks around Cg and CS are $T_{disk,Cg} \approx 159 \text{ yr}$ and $T_{disk,CS} \approx 186 \text{ yr}$. Assuming $M_{BHC6} + M_{BH4} \approx (M_{Cg} + M_{CS})/10 \approx 8 \cdot 10^7 M_{\odot}$, we have $M_{BHC6} \approx 8.7 \cdot 10^6 M_{\odot}$ and $M_{BH4} \approx 7.1 \cdot 10^7 M_{\odot}$. We find that the orbital period of the BBH system (BHC6-BH4) is $T_{bin} \approx 5130 \text{ yr}$, and the rotation period of the accretion disk around BHC6 is $T_{disk,Cg} \approx 152 \text{ yr}$. We can also find the orbital period of the two black hole systems, with a mean distance $\approx 1.35 \text{ mas}$, it is $T_{bin} \approx 46300 \text{ yr}$. We can deduce the propagation speeds of the different families of trajectories. The propagation speed of the family corresponding the ejection of C8 is $V_{a,Cg} \approx 0.045 \text{ c}$, the propagation speed of the family corresponding the ejection of C1 is $V_{a,CS} \approx 0.064 \text{ c}$ and the propagation speed of the family corresponding the ejection of C6 is $V_{a,BHC6} \approx 0.016 \text{ c}$.

During the period of observations, i.e. about 20 years, the black holes associated with CS and Cg ejected quasi regularly VLBI components but the second BBH system ejected only three components within 8 years (Fig. 5). Note that there is no periodicity for the ejection of VLBI components.

Kun et al. (2014) found that the flux density of first two mas of the VLBI jet was quasi periodic with a period $\approx 4.5 \text{ yr}$. The first two mas can contain VLBI components ejected by Cg and CS. The blue shift factor corresponding to component C1, ejected by CS, is ≈ 0.08 , and the blue shift factor corresponding to component C8, ejected by Cg, is ≈ 0.18 . The quasi period observed by Kun et al. (2014) was related to ejection of new VLBI components, and it corresponds, in the quasar frame, to a value between $\approx 25 \text{ yr}$ and $\approx 56 \text{ yr}$. This period corresponds to a fraction, i.e. between 1/8 and 1/3 of the rotation periods of the

accretion disks but does not correspond to the orbital period of the BBH system.

In the case of 1928+738, our modeling shows that the nucleus contains two BBH systems on the pc scale, i.e. the size of the binary systems are $R_{bin,1} \approx 0.22 \text{ mas} \approx 0.98 \text{ pc}$, $R_{bin,2} \approx 0.14 \text{ mas} \approx 0.62 \text{ pc}$, and the distance between the two BBH systems is $\approx 1.35 \text{ mas} \approx 6 \text{ pc}$. Deane et al. (2014) reports the detection of triple system which size is $\approx 7.4 \text{ kpc}$ with a binary system which size is $\approx 140 \text{ pc}$. The interpretation of Deane et al. (2014) has been questioned by Wrobel et al. (2014). For the formation of triple supermassive black hole systems, see Hoffman & Loeb (2007) and Kulkarni & Loeb (2012). As indicated in the Introduction, the ejection of VLBI components can be perturbed by the motion BBH system around a third black hole or an other BBH system. From VLBI observations there is a signature of this kind of perturbation, i.e. of the presence of a triple black hole system or a double BBH system in the nucleus. One observes close to the nucleus short period wiggles followed by a single turn which changes the ejection direction by a large angle, which can be 45 degrees. The best sources showing this behavior and which contains a triple system or two BBH systems are 3C 345 (work in progress) and 3C 454.3.

After the merging of two galaxies, if a BBH system form, it evolves *rapidly* to reach a critical radius $R_{bin} \sim 1 \text{ pc}$. After it loses energy emitting gravitational waves and it takes several billions years to collapse (Britzen et al. 2001). This explains that the typical size of the BBH system found in nuclei of extragalactic radio sources is $0.25 \text{ pc} \leq R_{bin} \leq 1.5 \text{ pc}$ (Roland 2014). A typical BBH system which size is $\approx 1 \text{ pc}$ and which contain two similar black holes of $10^8 M_{\odot}$ is characterized by an orbital period of 6600 yrs. The mean speed of the two black holes is $\approx 950 \text{ km/s}$. If the inclination angle of the source is $i_o \leq 10^\circ$, the difference between the radial speeds of the emission lines of the two cloud systems associated with the two black holes will be $\Delta V_r \leq 165 \text{ km/s}$. This result shows:

1. why it is difficult to detect BBH systems studying the broad lines spectra of quasars, and
2. the most efficient method to find BBH systems and to determine their characteristics is to study the kinematics of ejected VLBI components.

As shown in Fig. 7, the position of radio sources as measured by geodetic VLBI shows displacements larger than 0.1 mas in rms. This floor is obviously not only due to changes in the radio source structure: several other limiting factors like the mis-modeling of the troposphere wet delay and the noise introduced by site-dependent correlated errors play a non negligible role. In the case of 1928+738, the size of the BBH system associated with Cg and Cs is 0.22 mas and the distance between the two BBH systems is 1.35 mas. The corresponding coordinate time series (Fig. 8), computed after observations of the geodetic VLBI monitoring program of the International VLBI Service for Geodesy and Astrometry (IVS; Schuh & Behrend (2012); Lambert (2014)) is close to 0.3 mas, which is in agreement with (i) the size of the former BBH system, and (ii) the fact that this BBH system is much more active than the latter. For geodetic VLBI observations, 1928+738 therefore appears as a single BBH system of size 0.22 mas. However, the radio center detected by geodetic VLBI will follow the emitting black hole, and one can therefore expect significant displacements of the order of the size of the BBH system. Evidences of such a correspondence between the size of the BBH system, generally larger

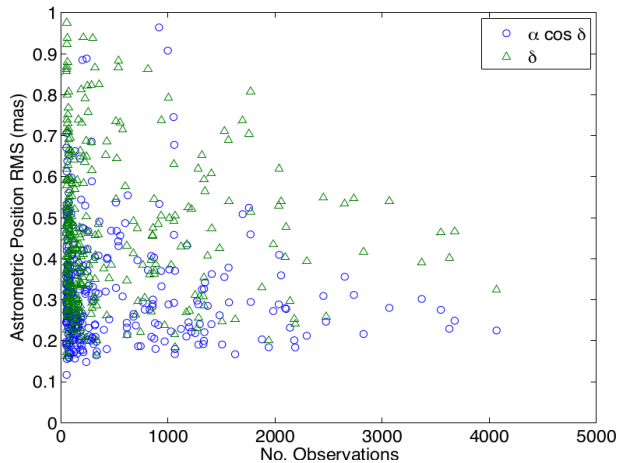


Fig. 7. Rms of the coordinate time series of the most observed quasars in the geodetic VLBI monitoring program of the International VLBI Service for Geodesy and Astrometry (IVS) (Lambert 2014) as a function of the number of sessions.

than 0.1 mas, and the rms of the coordinate time series has been raised in Roland (2014) although this study considered only a very few sources and must be extended to other sources. If so, it is likely that the astrometric precision of VLBI will be limited in the future by the size of the BBH systems, even at frequencies higher than the current 8.6 GHz band used for the ICRF2. The determination of the number and sizes of BBH systems in quasar nuclei will therefore be crucial in the future realization of reference frames, especially for the choice of the so-called defining sources that define the system axes and that should be, in principle, as point-like as possible.

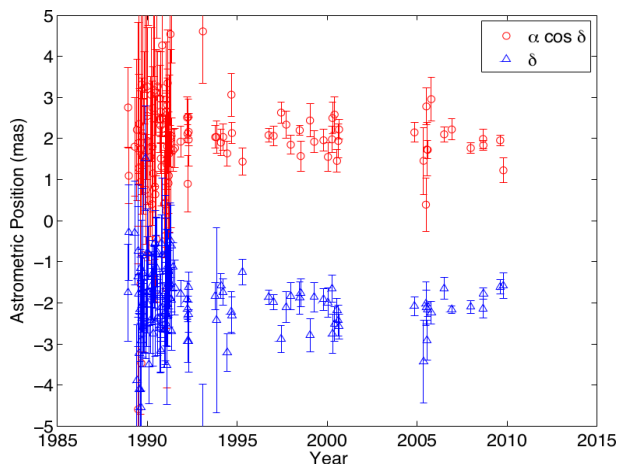


Fig. 8. Coordinate time series (mean removed and shifted by 2 mas for α and -2 mas for δ) of 1928+738 obtained by the analysis of data of the geodetic VLBI monitoring program of the IVS (Lambert 2014).

Same remarks can apply to the Gaia optical reference frame (Perryman et al. 2001). If the nucleus of the radio quasar contains a BBH system and if the two black holes are active, three different cases can happen:

1. the radio core and the optical core are associated with the same BH, then the distance between the radio core and the optical core depends on the opacity effect which will be small if the inclination angle is small,

2. the radio core and the optical core are associated with different black holes, then the distance between the radio core and the optical core is more or less the size of the BBH system (corrected by the possible opacity effect), and
3. the two black holes are emitting in the optical, then GAIA will provide a mean position between the two optical cores. This position will be different from the positions of the two radio cores.

As quasars are strongly and rapidly variables, during the 5 years of observations of GAIA, the 3 different cases can happen for a given source.

Although that in the case of 1928+738, it is associated with a bright optical quasar and the radio positions of the 2 radio emitting black holes are known,

- the large value of the inclination angle implies that opacity effect can be significant and
- the fact that the two black holes are active and ejecting VLBI components,

make the use of 1928+738 to obtain the precise link between the radio positions and the optical position, obtained by GAIA, difficult.

Acknowledgements. We thank the referee for very useful comments and one of us (JR) thanks Bertha Sese for enlightening discussions. This research has made use of data from the MOJAVE database that is maintained by the MOJAVE team (Lister et al. 2009a) and part of this work was supported by the COST Action MP0905 Black Holes in a Violent Universe.

References

- Begelman, M. C., Blandford, R. D., & Rees, M. J. 1980, *Nature*, 287, 307
- Britzen, S., Roland, J., Laskar, J., et al. 2001, *A&A*, 374, 784
- Colpi, M. & Dotti, M. 2011, *Advanced Science Letters*, 4, 181
- Deane, R. P., Paragi, Z., Jarvis, M. J., et al. 2014, *ArXiv e-prints*
- Fey, A. L., Gordon, D. G., Jacobs, C. S., & et al. 2009, in *Bundesamts für Kartographie und Geodäsie*, ed. Frankfurt am Main
- Healey, S. E., Romani, R. W., Cotter, G., et al. 2008, *ApJS*, 175, 97
- Hoffman, L. & Loeb, A. 2007, *MNRAS*, 377, 957
- Katz, J. I. 1997, *ApJ*, 478, 527
- Kelly, B. C. & Bechtold, J. 2007, *ApJS*, 168, 1
- Kulkarni, G. & Loeb, A. 2012, *MNRAS*, 422, 1306
- Kun, E., Gabányi, K. É., Karouzos, M., Britzen, S., & Gergely, L. Á. 2014, *MNRAS*, 445, 1370
- Lambert, S. 2013, *A&A*, 553, A122
- Lambert, S. 2014, in *Paris Observatory analysis center of the International VLBI Service for Geodesy and Astrometry (IVS)*, <http://ivsopar.obspm.fr>, personal communication
- Lawrence, C. R., Pearson, T. J., Readhead, A. C. S., & Unwin, S. C. 1986, *AJ*, 91, 494
- Lister, M. L., Aller, H. D., Aller, M. F., et al. 2009a, *AJ*, 137, 3718
- Lister, M. L., Aller, M. F., Aller, H. D., et al. 2013, *AJ*, 146, 120
- Lister, M. L., Cohen, M. H., Homan, D. C., et al. 2009b, *AJ*, 138, 1874
- Lister, M. L. & Homan, D. C. 2005, *AJ*, 130, 1389
- Lobanov, A. P. 1998, *A&A*, 330, 79
- Lobanov, A. P. & Roland, J. 2005, *A&A*, 431, 831
- Murphy, D. W., Browne, I. W. A., & Perley, R. A. 1993, *MNRAS*, 264, 298
- Perryman, M. A. C., de Boer, K. S., Gilmore, G., et al. 2001, *A&A*, 369, 339
- Roland, J. 2014, *ArXiv e-prints*
- Roland, J., Britzen, S., Caproni, A., et al. 2013, *A&A*, 557, A85
- Roland, J., Britzen, S., Kudryavtseva, N. A., Witzel, A., & Karouzos, M. 2008, *A&A*, 483, 125
- Roos, N., Kaastra, J. S., & Hummel, C. A. 1993, *ApJ*, 409, 130
- Schuh, H. & Behrend, D. 2012, *Journal of Geodyn.*, 61, 68
- Shepherd, M. C. 1997, in *Astronomical Society of the Pacific Conference Series*, Vol. 125, *Astronomical Data Analysis Software and Systems VI*, ed. G. Hunt & H. Payne, 77
- Wrobel, J. M., Walker, R. C., & Fu, H. 2014, *ApJ*, 792, L8

Appendix A: Fit of component C8

A.1. Introduction

The trajectory of C8 is observed for the first 5 mas, however the map of 1928+738 (Fig. 1) shows that the VLBI jet turns after about 10 mas (Lister & Homan 2005).

In a first step, we will try to find a solution of which could explain the long term turn using a BBH system, in a second step we will study the influence of a third black hole or a second BBH system on the solution and correct the coordinates of Kun et al. (2014) from this perturbation and finally determine the characteristics of the BBH system ejecting C8 using the corrected coordinates.

We used the method developed by Roland et al. (2008) and Roland et al. (2013).

A.2. Solution using the coordinates of Kun et al. (2014)

The solution obtained corresponds to a VLBI ejection which asymptotic direction is $\Delta\Xi \approx 182^\circ$.

The main characteristics of the BBH system ejecting C8 are that

- the two black holes are associated with the components CS and Cg,
- the VLBI component C8 is ejected by the VLBI core, i.e. component Cg (there is no indication of an offset of the origin of the ejection),
- the radius of the BBH system is $R_{bin} \approx 220 \mu\text{as} \approx 0.98 \text{ pc}$,
- the ratio M_{Cg}/M_{CS} is ≈ 4 , which is the inverse of the mass ratio found fitting the coordinates of C1 (Sec. D) and
- the ratio T_p/T_b is ≈ 129 .

The ratio M_{Cg}/M_{CS} is a free parameter of the model and the value $M_{Cg}/M_{CS} \approx 4$ comes from the fit of the coordinates of C8 (see Fig. A.1).

We find also that

- the inclination angle is $i_o \approx 26^\circ$,
- the angle between the accretion disk and the rotation plane of the BBH system is $\Omega \approx 9.2^\circ$,
- the bulk Lorentz factor of the VLBI component is $\gamma_c \approx 5.5$, and
- the origin of the ejection of the VLBI component is $t_o \approx 1993.9$.

The variations of the distance and the apparent speed of component C8 are showed in Fig. A.2. We find that component C8 moves with a mean apparent speed $v_{ap} \approx 4.1 c$, a value similar to that obtained by Lister et al. (2013).

The fits of the two coordinates $W(t)$ and $N(t)$ of the component C8 of 1928+738 are showed in Fig. A.3.

A.3. Determining the family of solutions

For the inclination angle previously found, i.e., $i_o \approx 26^\circ$, $T_p/T_b \approx 129$, $M_{Cg}/M_{CS} \approx 4$, and $R_{bin} \approx 220 \mu\text{as}$, we gradually varied V_a between 0.001 c and 0.45 c. The function $\chi^2(V_a)$ remained constant, indicating a degeneracy of the solution. We deduced the range of variation of the BBH system parameters. They are given in Table 4.

Table 4 : Ranges for the BBH system parameters ejecting C8

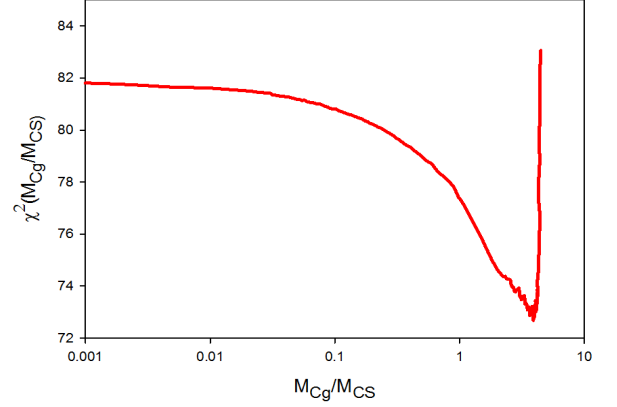


Fig. A.1. Determination of the parameter M_{Cg}/M_{CS} . We calculated $\chi^2(M_{Cg}/M_{CS})$ fitting of coordinates of C8, this provides the value of the ratio M_{Cg}/M_{CS} , i.e. $M_{Cg}/M_{CS} \approx 4$.

V_a	0.001 c	0.45 c
$T_p(V_a)$	$\approx 12000000 \text{ yr}$	$\approx 14000 \text{ yr}$
$T_b(V_a)$	$\approx 92000 \text{ yr}$	$\approx 108 \text{ yr}$
$(M_{Cg} + M_{CS})(V_a)$	$\approx 9.7 \cdot 10^5 M_\odot$	$\approx 7.0 \cdot 10^{11} M_\odot$

Table 4 provides the range of the BBH system parameters ejecting C8. To obtain the final range of the two BBH systems Cg-CS and BHC6-BH4 one has to make the intersection of the ranges of BBH systems parameters found after the fits of C8, C1 and C6 (see Sec. 8).

For $V_{a,Cg} = 0.1 c$, we find that the total mass of the BBH system ejecting C8 is $M_{Cg} + M_{CS} \approx 1.26 \times 10^{10} M_\odot$.

A.4. Determining the size of the accretion disk

From the knowledge of the mass ratio $M_{Cg}/M_{CS} \approx 4$ and the ratio $T_p/T_b \approx 130$, we calculated in the previous section the mass of the ejecting black hole M_{Cg} , the orbital period T_b , and the precession period T_p for each value of V_a .

The rotation period of the accretion disk, T_{disk} , is given by (2). Thus we calculated the rotation period of the accretion disk, and assuming that the mass of the accretion disk is $M_{disk} \ll M_{Cg}$, the size of the accretion disk is given by (3). We found that the size of the accretion disk does not depend on V_a and is $R_{disk} \approx 0.028 \text{ mas} \approx 0.124 \text{ pc}$.

Appendix B: Circular orbit correction of C8 coordinates

We found that the long term turn of the VLBI trajectory at about 10 mas could be explained by the BBH system associated with CS and Cg. However, components C5 and C6 are ejected by either a third black hole or a second BBH system, so we have to estimate the influence the slow rotation of the BBH system Cg-CS around the mass ejecting C5 and C6 and correct the coordinates of C8 from this perturbation to make a new determination of the characteristics of the BBH system ejecting C8.

Let us call M_{BH3} the mass ejecting C6, as the long term turn can be partly explained by the BBH system Cg-CS we should have $M_{BH3}/(M_{Cg} + M_{CS}) < 1$. We calculated the circular orbit correction for $M_{BH3}/(M_{Cg} + M_{CS}) = 1/10, 1$ and 10 and we found that we can find a non mirage solution only

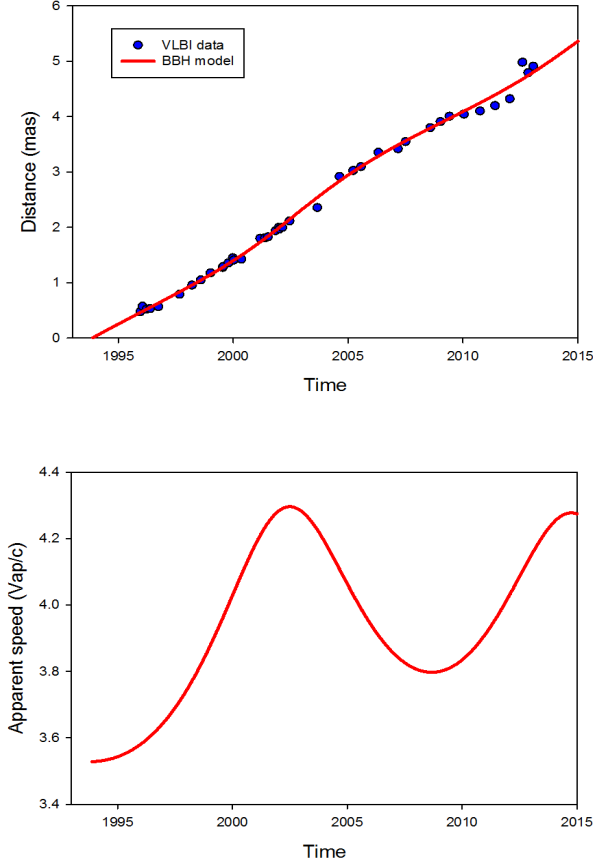


Fig. A.2. Variations of the distance and the apparent speed of component C8 assuming a constant bulk Lorentz factor $\gamma_c \approx 5.5$. *Top Figure:* From the plot of the variations of the distance we can deduce the mean speed: $4.86 \text{ mas} / 19.7 \text{ yr} \approx 247 \mu\text{s} / \text{yr}$. *Bottom Figure:* Although the large value of the inclination angle, we observe superluminal motion with a mean speed $\approx 4.1 c$.

if $M_{BH3}/(M_{Cg} + M_{CS}) < 1$. So to continue, we chosen arbitrarily the ratio $M_{BH3}/(M_{Cg} + M_{CS}) = 1/10$. In order to estimate the influence of the choice of this value on the final numerical result one could calculate the circular orbit correction assuming for instance $M_{BH3}/(M_{Cg} + M_{CS}) = 1/5$. This choice $M_{BH3}/(M_{Cg} + M_{CS}) = 1/5$ will not change the conclusion but simply the numerical result.

Using the parameters of the solution found in Sec. A, i.e. for $V_a = 0.1 c$, we have $M_{Cg} + M_{CS} \approx 1.26 \times 10^{10} M_\odot$ and then $M_{BH3} \approx 1.26 \times 10^9 M_\odot$. As the distance between the BBH system Cg-CS and BH3 is $\approx 1.35 \text{ mas}$ (see Sec. G), the corresponding orbital period of rotation of Cg-CS around BH3 is $T_{bin} \approx 11671 \text{ yr}$. Keeping the geometrical parameters of the solution found in Sec. A we calculate the trajectory and the tangent to the trajectory. At a given time, knowing the coordinates, $W_{CO}(t)$, $N_{CO}(t)$, of the trajectory of the VLBI component due to the slow circular orbit motion, and the coordinates, $W_{tan}(t)$, $N_{tan}(t)$, of the VLBI component along the tangent trajectory, the VLBI coordinates corrected from the slow orbital motion are

$$W_{cor}(t) = W(t) - (W_{CO}(t) - W_{tan}(t)), \quad (\text{B.1})$$

$$N_{cor}(t) = N(t) - (N_{CO}(t) - N_{tan}(t)). \quad (\text{B.2})$$

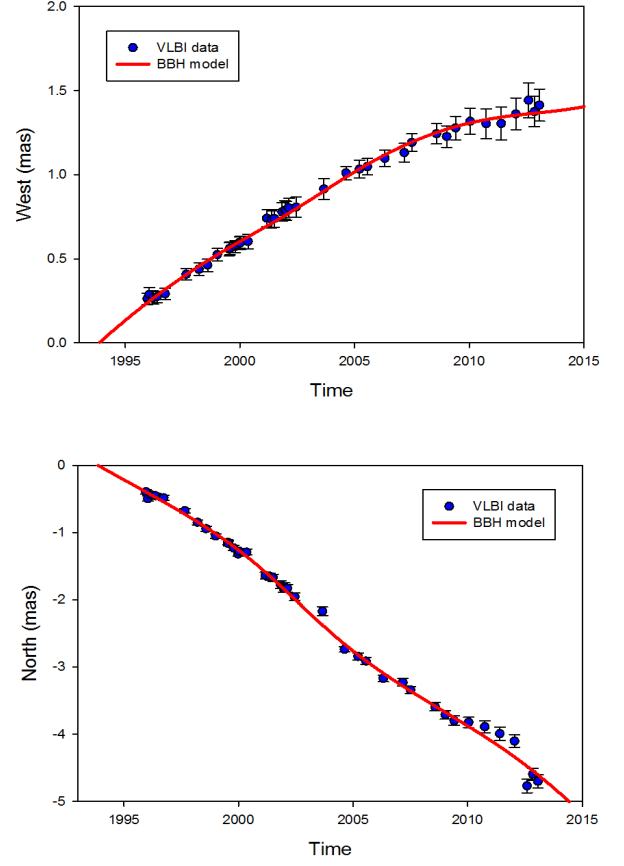


Fig. A.3. Fits of the two coordinates $W(t)$ and $N(t)$ of component C8 of 1928+738. They correspond to the solution with $T_p/T_b \approx 130$, $M_{Cg}/M_{CS} \approx 4$, and $i_o \approx 26^\circ$. The points are the observed coordinates of component C8. The VLBI coordinates and their error bars are taken from Kun et al. (2014). The red lines are the coordinates of the component trajectory calculated using the BBH model.

We plotted in Fig. B.1, the trajectory of the VLBI component due to the slow circular orbit motion, the tangent trajectory, the VLBI coordinates given by Kun et al. (2014) and the coordinates corrected from the slow orbital motion.

Using the corrected VLBI coordinates, we made a new determination of the characteristics of the BBH system ejecting component C8. The result is given in Sec. 5

Appendix C: Fit of component C7a

We assumed that component C7a belongs to the family of components ejected by the black hole Cg. To check this hypothesis and the consistency of the model found, we will use the characteristics of the BBH system Cg-CS and the characteristics of the geometrical parameters of the trajectory of C8, to fit the coordinates of components C7a.

If C7a has been ejected by Cg, we have to fit the coordinates of C7a using the characteristics of the BBH system Cg-CS found in Sec. A, i.e.

- Cg is the origin of the ejection,
- $T_p \approx 103998 \text{ yr}$,
- $T_p/T_b \approx 129$,
- $R_{bin} \approx 0.220 \mu\text{s}$ and

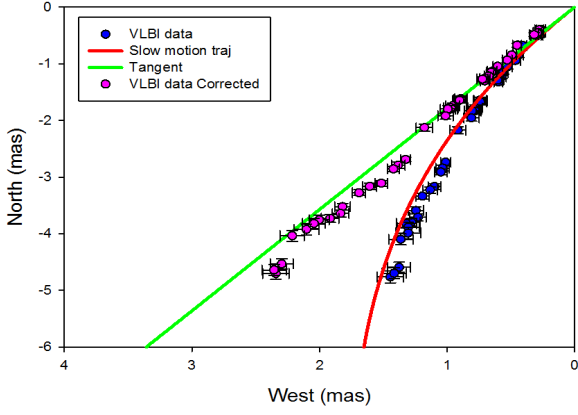


Fig. B.1. Plot of the trajectory of the VLBI component due to the slow circular orbit motion, the tangent trajectory, the VLBI coordinates given by Kun et al. (2014) and the coordinates corrected from the slow orbital motion.

$$- M_{Cg}/M_{CS} \approx 4,$$

and using the same geometrical parameters than those found to fit the trajectory of C8, i.e.

- $\Delta\Xi \approx 182^\circ$,
- $\Omega \approx 9.2^\circ$,
- $R_o \approx 28$ pc and
- $T_d \approx 710$ yr.

Then we calculate $\chi^2(i_o)$ starting from $i_o \approx 26^\circ$ and assuming that the parameters:

- ϕ_o the phase of the precession at t_o ,
- γ_c the bulk Lorentz,
- Ψ_o the phase of the BBH system at t_o and
- t_o the time origin of the ejection of the component,

are free parameters.

The best fit is obtained for $i_o \approx 20^\circ$. The bulk Lorentz factor is $\gamma \approx 4.1$ and the time origin of the ejection is $t_o \approx 1992$. The trajectory of C7a is shown in Fig. C.1. We obtain a very good fit of each coordinate showing that

- component C7a has been ejected by Cg,
- the characteristics of the BBH system Cg-CS are correct and
- the solution found for the ejection of component C8 is the correct one.

Appendix D: Fit of component C1

The solution obtained corresponds to a VLBI ejection which asymptotic direction is $\Delta\Xi \approx 182^\circ$.

The main characteristics of the solution of the BBH system associated with 1928+738 are that

- the VLBI component C1 is not ejected by the VLBI core Cg, but by component CS (there is a weak indication of an offset of the origin of the ejection in the direction of CS, this weak indication is due to the lack of observations of C1 for the beginning of the trajectory),
- the coordinates of CS are $X_{CS} \approx -0.07$ mas and $Y_{CS} \approx +0.21$ mas,

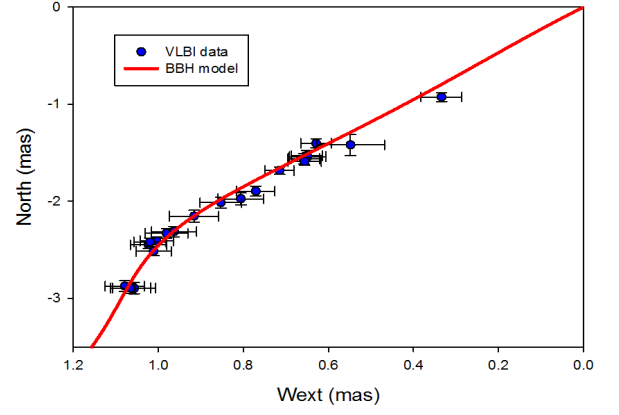


Fig. C.1. Trajectory of C7a assuming that it has been ejected by the black hole Cg of the BBH system Cg-CS and using the characteristics of the BBH system Cg-CS obtained during the fit of component C8 and the geometrical parameters of the trajectory of C8.

- the radius of the BBH system is $R_{bin} \approx 220 \mu\text{as} \approx 0.98$ pc,
- the ratio $M_{CS}/M_{Cg} \approx 1/4$, which is the inverse of the mass ratio found fitting the coordinates of C8 (Sec. A) and
- the ratio T_p/T_b is ≈ 53 .

The ratio M_{CS}/M_{Cg} is a free parameter of the model and the value $M_{CS}/M_{Cg} \approx 0.25$ comes from the fit of the coordinates of C1 (see Fig. D.1). The fact that the fit of C1 provides a mass ratio $M_{CS}/M_{Cg} \approx 0.25$ which is the inverse of the mass ratio $M_{Cg}/M_{CS} \approx 4$ obtained from the fit of component C8 shows that components C1 and C8 are not ejected by the same black hole.

We find that

- the inclination angle is $i_o \approx 23^\circ$,
- the angle between the accretion disk and the rotation plane of the BBH system is $\Omega \approx 10.3^\circ$,
- the bulk Lorentz factor of the VLBI component is $\gamma_c \approx 5.9$, and
- the origin of the ejection of the VLBI component is $t_o \approx 1967$.

The variations of the distance and the apparent speed of component C1 are showed in Fig. D.2. We find that component C1 moves with a mean apparent speed $v_{ap} \approx 4.7c$, a value smaller than the one obtained by Lister et al. (2013).

The fit of the two coordinates $W(t)$ and $N(t)$ of the component C1 of 1928+738 is showed in Fig. D.3. The points are the observed coordinates of component C1 that were corrected by the offsets $\Delta W \approx -70 \mu\text{as}$ and $\Delta N \approx +210 \mu\text{as}$, and the red lines are the coordinates of the component trajectory calculated using the BBH model.

D.1. Determining the family of solutions

For the inclination angle previously found, i.e., $i_o \approx 23^\circ$, $T_p/T_b \approx 53$, $M_{CS}/M_{Cg} \approx 1/4$, and $R_{bin} \approx 220 \mu\text{as}$, we gradually varied V_a between 0.001 c and 0.45 c. The function $\chi^2(V_a)$ remained constant, indicating a degeneracy of the solution. We deduced the range of variation of the BBH system parameters. They are given in Table 5.

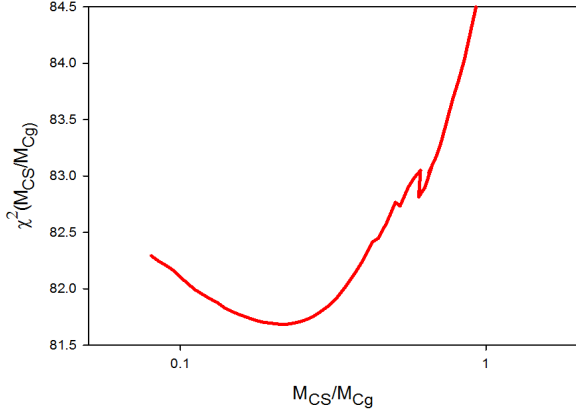


Fig. D.1. Determination of the parameter M_{CS}/M_{Cg} . We calculated $\chi^2(M_{CS}/M_{Cg})$ fitting of coordinates of C1, this provides the value of the ratio M_{CS}/M_{Cg} , i.e. $M_{CS}/M_{Cg} \approx 0.25$.

Table 5 : Ranges for the BBH system parameters ejecting C1

V_a	0.001 c	0.45 c
$T_p(V_a)$	≈ 12400000 yr	≈ 14900 yr
$T_b(V_a)$	≈ 230000 yr	≈ 279 yr
$(M_{Cg} + M_{CS})(V_a)$	$\approx 1.5 \cdot 10^5 M_\odot$	$\approx 1.0 \cdot 10^{11} M_\odot$

Table 5 provides the range of the BBH system parameters ejecting C1. To obtain the final range of the two BBH systems Cg-CS and BHC6-BH4 one has to make the intersection of the ranges of BBH systems parameters found after the fits of C8, C1 and C6 (see Sec. 8).

For $V_{a,CS} = 0.1 c$, we find that the total mass of the BBH system ejecting C1 is $M_{Cg} + M_{CS} \approx 1.87 \times 10^9 M_\odot$. The total mass of the BBH system ejecting C1 is the same that the total mass of the BBH system ejecting C8 if $V_{a,CS} \approx 0.232 c$, i.e. the propagation speeds of the perturbations are different for different families of trajectories (see Sec. 8 for the determination of the propagation speeds of the perturbations of three families of trajectories if $M_{Cg} + M_{CS} \approx 8 \times 10^8 M_\odot$).

D.2. Determining the size of the accretion disk

From the knowledge of the mass ratio $M_{CS}/M_{Cg} \approx 1/4$ and the ratio $T_p/T_b \approx 53$, we calculated in the previous section the mass of the ejecting black hole M_{CS} , the orbital period T_b , and the precession period T_p for each value of V_a .

The rotation period of the accretion disk, T_{disk} , is given by (2). Thus we calculated the rotation period of the accretion disk, and assuming that the mass of the accretion disk is $M_{disk} \ll M_{CS}$, the size of the accretion disk is given by (3). We found that the size of the accretion disk, does not depend on V_a and is $R_{disk} \approx 0.013 \text{ mas} \approx 0.058 \text{ pc}$.

Appendix E: Circular orbit correction of C1 coordinates

We calculated the circular orbit correction for $M_{Cg} + M_{CS} = 10 * (M_{BHC6} + M_{BH4})$.

Using the parameters of the solution found in Sec. D, i.e. for $V_a = 0.1 c$, we have $M_{Cg} + M_{CS} \approx 1.9 \times 10^9 M_\odot$ and then $M_{BHC6} + M_{BH4} \approx 1.9 \times 10^8 M_\odot$. As the distance between the

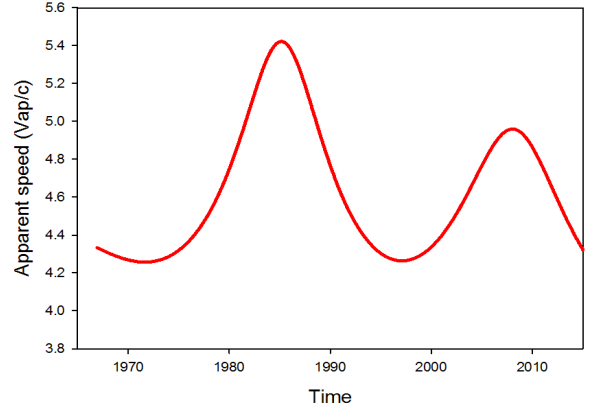
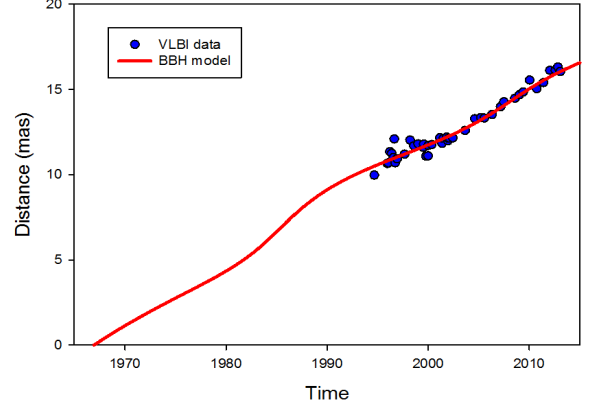


Fig. D.2. Variations of the distance and the apparent speed of component C1 assuming a constant bulk Lorentz factor $\gamma_c \approx 5.9$. *Top Figure:* From the plot of the variations of the distance we can deduce the mean speed: $16 \text{ mas} / 46 \text{ yr} \approx 350 \mu\text{s} / \text{yr}$. *Bottom Figure:* Although the large value of the inclination angle, we observe superluminal motion with a mean speed $\approx 4.7 c$.

two BBH systems is $\approx 1.35 \text{ mas}$ (see Sec. G), the corresponding orbital period of rotation of Cg-CS around BHC6-BH4 is $T_{bin} \approx 30320 \text{ yr}$. Keeping the geometrical parameters of the solution found in Sec. D we calculate the trajectory and the tangent to the trajectory. At a given time, knowing the coordinates, $W_{CO}(t)$, $N_{CO}(t)$, of the trajectory of the VLBI component due to the slow circular orbit motion, and the coordinates, $W_{tan}(t)$, $N_{tan}(t)$, of the VLBI component along the tangent trajectory, the VLBI coordinates corrected from the slow orbital motion are given by equations (B.1) and (B.2).

We plotted in Fig. E.1, the trajectory of the VLBI component due to the slow circular orbit motion, the tangent trajectory, the VLBI coordinates given by Kun et al. (2014) and the coordinates corrected from the slow orbital motion.

Using the corrected VLBI coordinates, we made a new determination of the characteristics of the BBH system ejecting component C1. The result is given in Sec. 6

Appendix F: Fit of component C9

We assumed that component C9 belongs to the family of components ejected by the black hole CS. To check this hypothesis and the consistency of the model found, we will use the characteristics of the BBH system Cg-CS and the characteristics of the

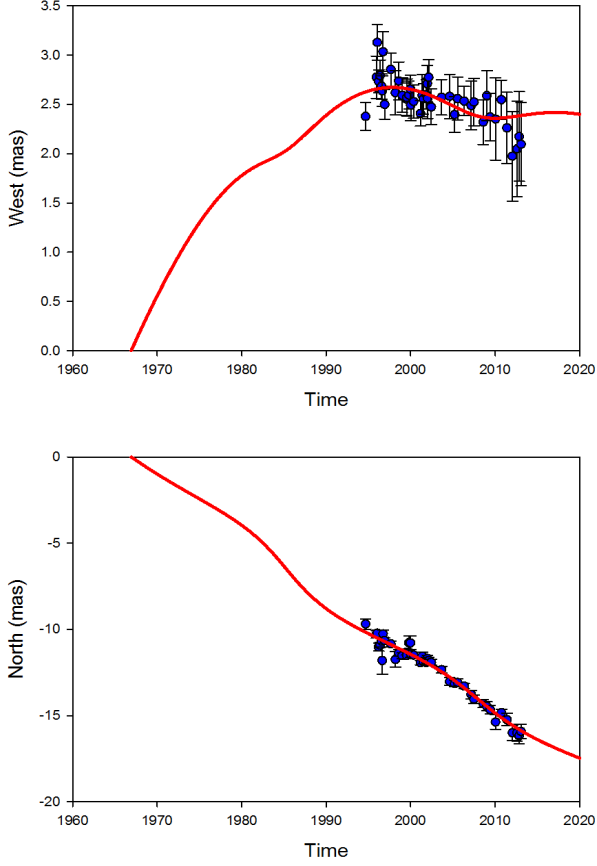


Fig. D.3. Fit of the two coordinates $W(t)$ and $N(t)$ of component C1 of 1928+738. They correspond to the solution with $T_p/T_b \approx 53$, $M_{CS}/M_{Cg} \approx 1/4$, and $i_o \approx 23^\circ$. The points are the observed coordinates of component C1 that were corrected by the offsets $\Delta W \approx -70 \mu\text{as}$ and $\Delta N \approx +210 \mu\text{as}$. The VLBI coordinates and their error bars are taken from Kun et al. (2014). The red lines are the coordinates of the component trajectory calculated using the BBH model.

geometrical parameters of the trajectory of C1, to fit the coordinates of components C9.

If C9 has been ejected by CS, we have to fit the coordinates of C9 using the characteristics of the BBH system Cg-CS found in Sec. D, i.e.

- CS is the origin of the ejection,
- $T_p \approx 101866$ yr,
- $T_p/T_b \approx 53$,
- $R_{bin} \approx 0.220 \mu\text{as}$ and
- $M_{CS}/M_{Cg} \approx 0.25$,

and using the same geometrical parameters than those found to fit the trajectory of C1, i.e.

- $\Delta E \approx 182^\circ$,
- $\Omega \approx 10.3^\circ$,
- $R_o \approx 56$ pc and
- $T_d \approx 1278$ yr.

To begin, the coordinates of C9 given by (Kun et al. 2014) are corrected by the offsets $\Delta X_{C9} \approx -0.07$ mas and $\Delta Y_{C9} \approx +0.21$ mas.

Then we calculate $\chi^2(i_o)$ starting from $i_o \approx 23^\circ$ and assuming that the parameters:

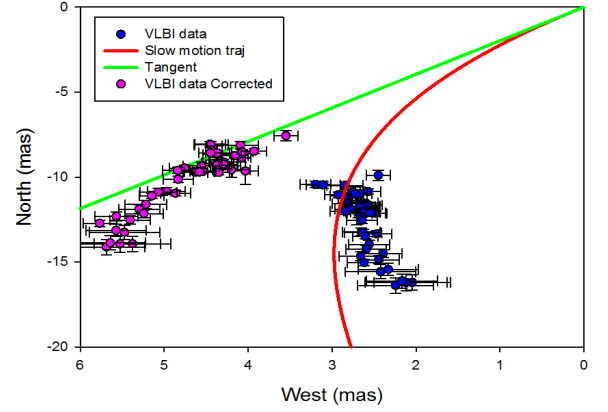


Fig. E.1. Plot of the trajectory of the VLBI component due to the slow circular orbit motion, the tangent trajectory, the VLBI coordinates given by Kun et al. (2014) and the coordinates corrected from the slow orbital motion.

- ϕ_o the phase of the precession at t_o ,
- γ_c the bulk Lorentz,
- Ψ_o the phase of the BBH system at t_o and
- t_o the time origin of the ejection of the component,

are free parameters.

The best fit is obtained for $i_o \approx 20^\circ$. The bulk Lorentz factor is $\gamma \approx 4.3$ and the time origin of the ejection is $t_o \approx 1993.3$. The trajectory of C9 is shown in Fig. F.1. We obtain a very good fit of each coordinate showing that

- component C9 has been ejected by CS,
- the characteristics of the BBH system Cg-CS are correct and
- the solution found for the ejection of component C1 is the correct one.

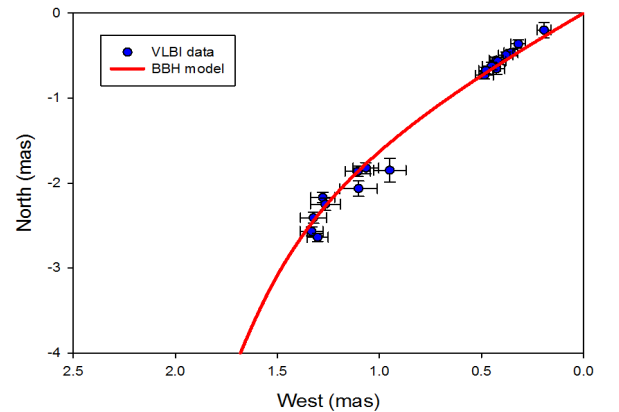


Fig. F.1. Trajectory of C9 assuming that it has been ejected by the black hole CS of the BBH system Cg-CS and using the characteristics of the BBH system Cg-CS obtained during the fit of component C1 and the geometrical parameters of the trajectory of C1.

Appendix G: Fit of component C6

The component C6 is not ejected by CS or Cg but is ejected by a third black hole. We can show that this third black hole belongs to a second BBH system. Indeed, if we assume that C6 is ejected by a single black hole, we applied the precession model and we studied the solution $\chi^2(i_o)$ in the interval $2^\circ \leq i_o \leq 50^\circ$, we found that

1. there exist solutions with $\gamma < 30$ only in the interval $2^\circ \leq i_o \leq 17^\circ$ (see Fig. G.1),
2. the solution with $\gamma < 30$ is a mirage solution, i.e. the curve $\chi^2(i_o)$ is convex and it does not show a minimum; moreover the bulk Lorentz factor γ diverges when $i_o \rightarrow 17^\circ$ (see Fig. G.2) and
3. the precession period corresponding to the solution is: 1200 yr $\leq T_{prec} \leq 2000$ yr. This precession period too small to be explained by either the Lense-Thirring effect, i.e. a spinning black hole or the precession due to the rotation of the black hole ejecting C6 around the BBH system Cg-CS.

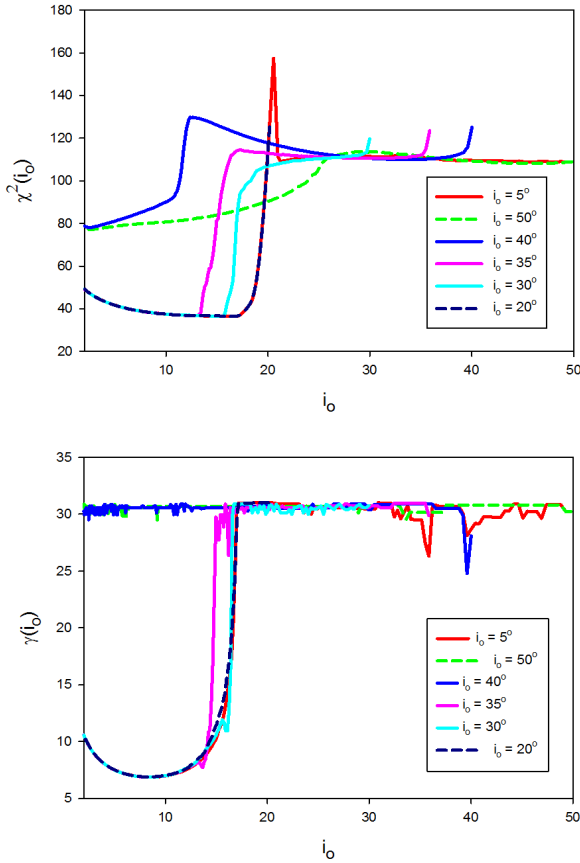


Fig. G.1. Assuming that component C6 is ejected by a single black hole, we applied the precession model and we calculated $\chi^2(i_o)$ in the interval $2^\circ \leq i_o \leq 50^\circ$ starting from 6 different values of the inclination angle, namely $i_o = 5^\circ, 50^\circ, 40^\circ, 35^\circ, 30^\circ$ and 20° . We found that there exist solutions with $\gamma < 30$ only in the interval $2^\circ \leq i_o \leq 17^\circ$. *Top Figure:* The curves $\chi^2(i_o)$ calculated starting from 6 different values of the inclination angle. *Bottom Figure:* The corresponding bulk Lorentz factor γ .

However, if the black hole ejecting C6 belongs to a second BBH system, the corresponding solution is no longer a mirage

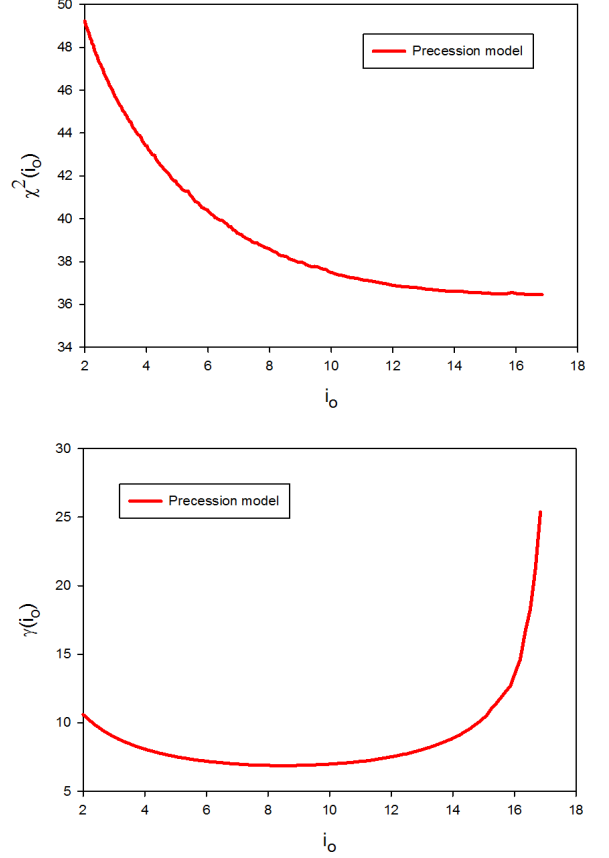


Fig. G.2. Assuming that component C6 is ejected by a single black hole, we applied the precession model and the solution with $\gamma < 30$ is a mirage solution, i.e. the curve $\chi^2(i_o)$ is convex and it does not show a minimum; moreover the bulk Lorentz factor γ diverges when $i_o \rightarrow 17^\circ$. *Top Figure:* The curve $\chi^2(i_o)$ is convex and it does not show a minimum. *Bottom Figure:* The bulk Lorentz factor γ diverges when $i_o \rightarrow 17^\circ$.

solution, i.e. the curve $\chi^2(i_o)$ is concave and shows a minimum. We will call BHC6 the black hole ejecting component C6 and BH4 the second black hole of the second BBH system.

In this section we present the characteristics of the BBH system BHC6-BH4 using the coordinates of C6 given by (Kun et al. 2014).

The main characteristics of the solution of the BBH system ejecting C6 are that

- the coordinates of BHC6 are $X_{BHC6} \approx -0.11$ mas and $Y_{BHC6} \approx -1.30$ mas (assuming that the origin is associated with Cg),
- none of the two black holes are associated with a stationary VLBI component, i.e. they are not strong sources,
- the radius of the BBH system is $R_{bin} \approx 140 \mu\text{as} \approx 0.62 pc$,
- calling M_{BHC6} the mass of the black hole ejecting C6 and M_{BH4} the mass of the other black hole, the ratio M_{BHC6}/M_{BH4} is ≈ 0.3 , and
- the ratio T_p/T_b is ≈ 1456 .

We find that

- the inclination angle is $i_o \approx 21^\circ$,

- the angle between the accretion disk and the rotation plane of the BBH system is $\Omega \approx 3.6^\circ$,
- the bulk Lorentz factor of the VLBI component is $\gamma_c \approx 4.6$, and
- the time origin of the ejection of the VLBI component is $t_o \approx 1994.7$.

The variations of the distance and the apparent speed of component C6 are showed in Fig. G.3. We find that component C6 moves with a mean apparent speed $v_{ap} \approx 4.4 c$, a value comparable to the one obtained by Lister et al. (2013).

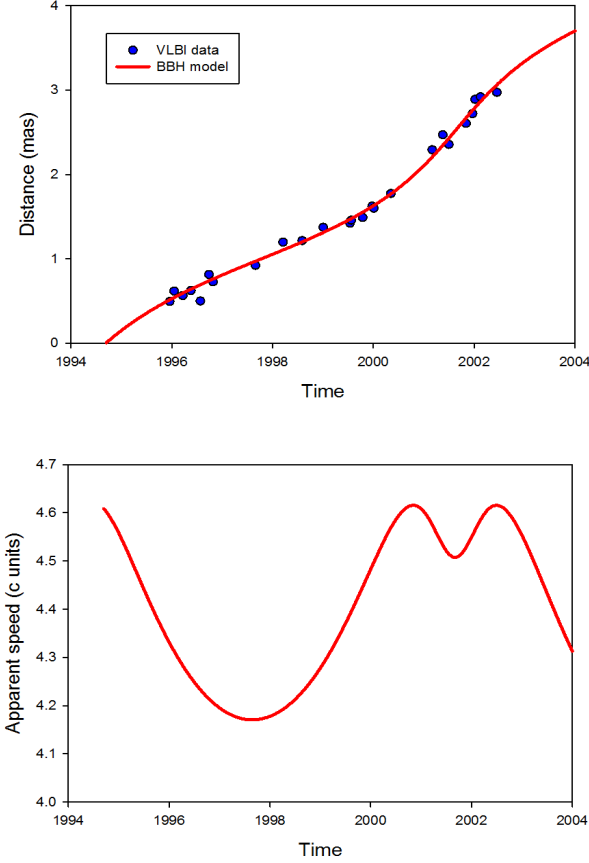


Fig. G.3. Variations of the distance and the apparent speed of component C6 assuming a constant bulk Lorentz factor $\gamma_c \approx 4.6$. *Top Figure:* From the plot of the variations of the distance we can deduce the mean speed: $3 \text{ mas} / 7.8 \text{ yr} \approx 385 \mu\text{as} / \text{yr}$. *Bottom Figure:* Although the large value of the inclination angle, we observe superluminal motion with a mean speed $\approx 4.4 c$.

The fit of the two coordinates $W(t)$ and $N(t)$ of the component C6 of 1928+738 is showed in Fig. G.4. The points are the observed coordinates of component C6 that were corrected by the offsets $\Delta W \approx +110 \mu\text{as}$ and $\Delta N \approx +1300 \mu\text{as}$, and the red lines are the coordinates of the component trajectory calculated using the BBH model.

G.1. Determining the family of solutions

For the inclination angle previously found, i.e., $i_o \approx 21^\circ$, $T_p/T_b \approx 1500$, $M_{BHC6}/M_{BH4} \approx 0.3$, and $R_{bin} \approx 140 \mu\text{as}$, we gradually varied V_a between $0.001 c$ and $0.45 c$. The function

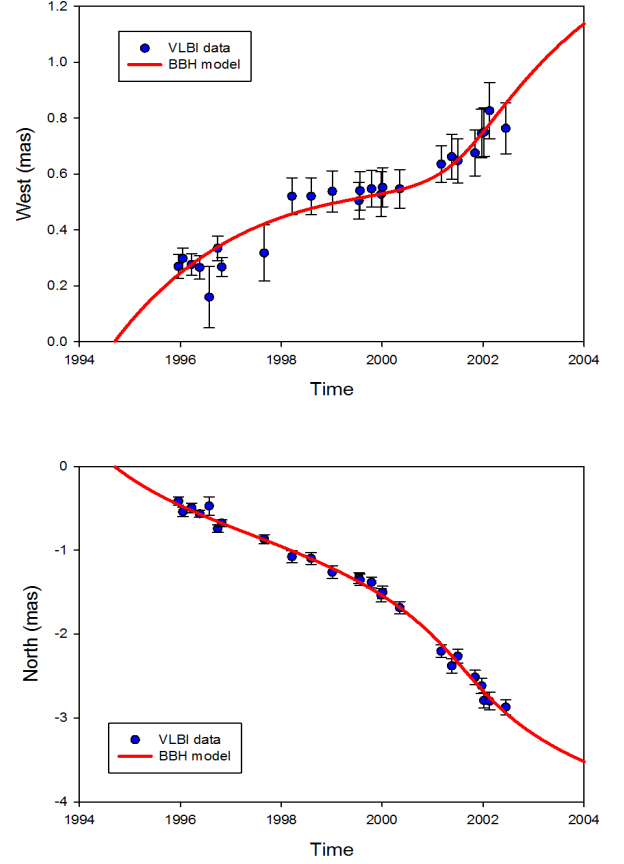


Fig. G.4. Fit of the two coordinates $W(t)$ and $N(t)$ of component C6 of 1928+738. They correspond to the solution with $T_p/T_b \approx 1500$, $M_{BHC6}/M_{BH4} \approx 0.3$, and $i_o \approx 21^\circ$. The points are the observed coordinates of component C6 that were corrected by the offsets $\Delta W \approx +110 \mu\text{as}$ and $\Delta N \approx +1300 \mu\text{as}$. The VLBI coordinates and their error bars are taken from Kun et al. (2014). The red lines are the coordinates of the component trajectory calculated using the BBH model.

$\chi^2(V_a)$ remained constant, indicating a degeneracy of the solution. We deduced the range of variation of the BBH system parameters. They are given in Table 6.

Table 6 : Ranges for the BBH system parameters ejecting C6

V_a	$0.001 c$	$0.45 c$
$T_p(V_a)$	$\approx 149000000 \text{ yr}$	$\approx 179500 \text{ yr}$
$T_b(V_a)$	$\approx 102500 \text{ yr}$	$\approx 123 \text{ yr}$
$(M_{Cg} + M_{CS})(V_a)$	$\approx 2 \cdot 10^5 M_\odot$	$\approx 1.4 \cdot 10^{11} M_\odot$

Table 6 provides the range of the BBH system parameters ejecting C6. To obtain the final range of the two BBH systems Cg-CS and BHC6-BH4 one has to make the intersection of the ranges of BBH systems parameters found after the fits of C8, C1 and C6 (see Sec. 8).

For $V_{a,CS} = 0.1 c$, we find that the total mass of the BBH system ejecting C1 is $M_{Cg} + M_{CS} \approx 1.87 \times 10^9 M_\odot$. The total mass of the BBH system ejecting C6 is $M_{BHC6} + M_{BH4} = (M_{Cg} + M_{CS})/10$ if $V_{a,BHC6} \approx 0.030 c$, i.e. the propagation speeds of the perturbations are different for different families of trajectories (see Sec. 8 for the determination of the propagation speeds of the perturbations of three families of trajectories if $M_{Cg} + M_{CS} \approx 8 \times 10^8 M_\odot$).

G.2. Determining the size of the accretion disk

From the knowledge of the mass ratio $M_{BHC6}/M_{BH4} \approx 0.3$ and the ratio $T_p/T_b \approx 1500$, we calculated in the previous section the mass of the ejecting black hole M_{BHC6} , the orbital period T_b , and the precession period T_p for each value of V_a .

The rotation period of the accretion disk, T_{disk} , is given by (2). Thus we calculated the rotation period of the accretion disk, and assuming that the mass of the accretion disk is $M_{disk} \ll M_{BHC6}$, the size of the accretion disk is given by (3). We found that the size of the accretion disk, does not depend on V_a and is $R_{disk} \approx 0.00096 \text{ mas} \approx 0.0043 \text{ pc}$.

Appendix H: Circular orbit correction of C6 coordinates

We calculated the circular orbit correction for $M_{BHC6} + M_{BH4} = (M_{Cg} + M_{CS})/10$.

Using the parameters of the solution found in Sec. G, i.e. for $V_{a,C6} = 0.1 \text{ c}$, the mass of the BBH system ejecting C6 is $M_{BHC6} + M_{BH4} \approx 2.5 \times 10^9 M_\odot$ and then $M_{Cg} + M_{CS} \approx 2.5 \times 10^{10} M_\odot$. We could calculate the circular orbit correction for a different value of V_a to have a mass $M_{Cg} + M_{CS}$ equal to the mass used in Sec. B, however due to the degeneracy of the solution the result will be the same.

The distance between the two BBH systems is $\approx 1.35 \text{ mas}$ (see Sec. G), the corresponding orbital period of rotation of Cg-CS around BHC6-BH4 is $T_{bin} \approx 8837 \text{ yr}$. Keeping the geometrical parameters of the solution found in Sec. G we calculate the trajectory and the tangent to the trajectory. At a given time, knowing the coordinates, $W_{CO}(t)$, $N_{CO}(t)$, of the trajectory of the VLBI component due to the slow circular orbit motion, and the coordinates, $W_{tan}(t)$, $N_{tan}(t)$, of the VLBI component along the tangent trajectory, the VLBI coordinates corrected from the slow orbital motion are given by equations (B.1) and (B.2).

We plotted in Fig. H.1, the trajectory of the VLBI component due to the slow circular orbit motion, the tangent trajectory, the VLBI coordinates given by Kun et al. (2014) and the coordinates corrected from the slow orbital motion.

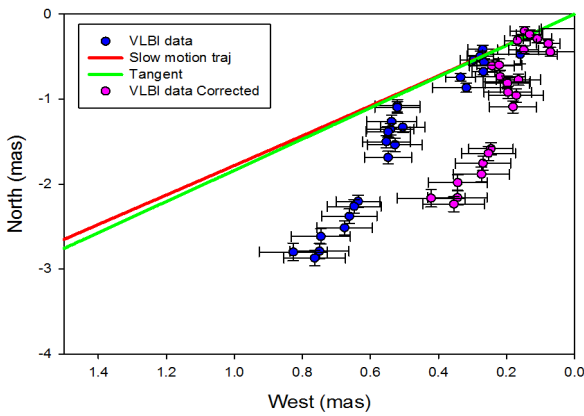


Fig. H.1. Plot of the trajectory of the VLBI component due to the slow circular orbit motion, the tangent trajectory, the VLBI coordinates given by Kun et al. (2014) and the coordinates corrected from the slow orbital motion.

Using the corrected VLBI coordinates, we made a new determination of the characteristics of the BBH system ejecting component C6. The result is given in Sec. 7.

Appendix I: Fit of component C5

We assumed that component C5 belongs to the family of components ejected by the black hole BHC6. To check this hypothesis and the consistency of the model found, we will use the characteristics of the BBH system BHC6-BH4 and the characteristics of the geometrical parameters of the trajectory of C6, to fit the coordinates of components C5.

If C5 has been ejected by BHC6, we have to fit the coordinates of C5 using the characteristics of the BBH system BHC6-BH4 found in Sec. G, i.e.

- BHC6 is the origin of the ejection,
- $T_p \approx 1344545 \text{ yr}$,
- $T_p/T_b \approx 1456$,
- $R_{bin} \approx 0.140 \mu\text{as}$ and
- $M_{BHC6}/M_{BH4} \approx 0.3$,

and using the same geometrical parameters than those found to fit the trajectory of C6, i.e.

- $\Delta\Xi \approx 165^\circ$,
- $\Omega \approx 3.6^\circ$,
- $R_o \approx 103 \text{ pc}$ and
- $T_d \approx 1500 \text{ yr}$.

To begin, the coordinates of C5 given by (Kun et al. 2014) are corrected by the offsets $\Delta X_{C5} \approx +0.10 \text{ mas}$ and $\Delta Y_{C5} \approx +1.30 \text{ mas}$.

Then we calculate $\chi^2(i_o)$ starting from $i_o \approx 21^\circ$ and assuming that the parameters:

- ϕ_o the phase of the precession at t_o ,
- γ_c the bulk Lorentz,
- Ψ_o the phase of the BBH system at t_o and
- t_o the time origin of the ejection of the component,

are free parameters.

The best fit is obtained for $i_o \approx 20^\circ$. The bulk Lorentz factor is $\gamma \approx 4.3$ and the time origin of the ejection is $t_o \approx 1991$. The trajectory of C5 is shown in Fig. I.1. We obtain a very good fit of each coordinate showing that

- component C5 has been ejected by BHC6,
- the characteristics of the BBH system BHC6-BH4 are correct and
- the solution found for the ejection of component C6 is the correct one.

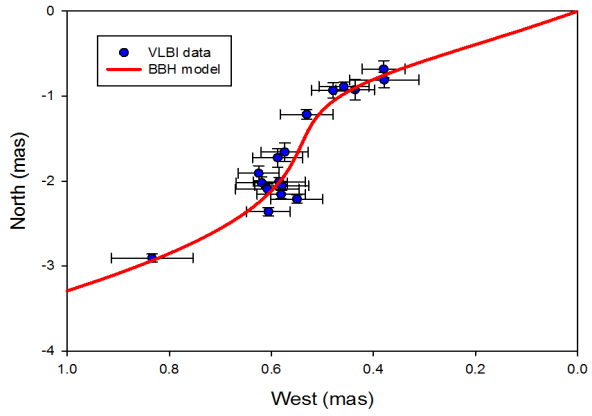


Fig. I.1. Trajectory of C5 assuming that it has been ejected by the black hole BHC6 of the BBH system BHC6-BH4 and using the characteristics of the BBH system BHC6-BH4 obtained during the fit of component C6 and the geometrical parameters of the trajectory of C6.